Harmful Algae 104 (2021) 101956

Contents lists available at ScienceDirect

Harmful Algae

journal homepage: www.elsevier.com/locate/hal

Recommendations for epitypification of dinophytes exemplified by *Lingulodinium polyedra* and molecular phylogenetics of the Gonyaulacales based on curated rRNA sequence data

Urban Tillmann [a], Alexis Bantle [a], Bernd Krock [a], Malte Elbrächter [b], Marc Gottschling [c,*]

[a] *Alfred-Wegener-Institute, Helmholtz Centre for Polar and Marine Research, Am Handelshafen 12, D – 27 570 Bremerhaven, Germany*
[b] *Alfred-Wegener-Institute, Helmholtz Centre for Polar and Marine Research, Sylt, Hafenstr. 43, D – 25 992 List/Sylt, Germany*
[c] *Department Biologie, Systematische Botanik und Mykologie, GeoBio-Center, Ludwig-Maximilians-Universität München, Menzinger Str. 67, D – 80 638 München, Germany*

A B S T R A C T

Gonyaulacales include a considerable number of harmful algae and to understand their origin and rise, knowledge of the evolutionary relationships is necessary. Many scientific names of protists introduced prior to the availability of DNA analytics are ambiguous and impede communication about biological species and their traits in the microbial world. Strains of *Lingulodinium polyedra* were established from its type locality in the Kiel Fjord (Germany) to clarify its taxonomy. Moreover, the phylogeny of Gonyaulacales was inferred based on 329 rRNA sequence accessions compiled in a curated sequence data base, with as much as possible type material equivalents included. Gonyaulacales were monophyletic and segregated into seven lineages at high systematic level, of which †Lingulodiniaceae constituted the first branch of the Gonyaulacales. Their type species had a plate formula APC (Po, X, cp), 3′, 3a, 6′′ 6c, 6s, 6′′′, 2′′′′ and is taxonomically clarified by epitypification. Recommendations for this important taxonomic tool are provided, with a focus on microorganisms. Most gonyaulacalean taxa established at generic rank are monophyletic, with *Alexandrium, Coolia* and *Gonyaulax* as notable exceptions. From an evolutionary perspective, gonyaulacalean dinophytes with quinqueform hypotheca are monophyletic and derive from a paraphyletic group showing the sexiform configuration.

1. Introduction

More than a century ago, Stein (1883: 13, pl. IV 7–9) described the gonyaulacalean dinophyte *Lingulodinium* (≡ *Gonyaulax*) *polyedra* (F. Stein) J.D.Dodge from the Baltic Sea off Kiel (Germany), probably collected in late summer 1879 (Wentzel, 1885). It is worthy to note that F. von Stein found the algal remnants in the digestion tracts of ascidiacean tunicates, described under the zoological code of nomenclature (Gottschling et al., 2018) and provided an illustration with analysis (ICN Art. 38.8). His minute illustrations show heavily armoured cells with an obtusely heptagonal shape in outline and a porate surface (here reproduced as Fig. 1). A distinct pattern of cellulosic plates is present, which comprise nine epithecal and seven bigger hypothecal plates in F. v. Stein's figure. *Lingulodinium polyedra* is bioluminescent (Haxo and Sweeney, 1955; Schmitter, 1971) and was the Algae of the Year 2013 (Phycology Section in the German Society for Plant Sciences: DBG).

Lingulodinium polyedra has an interesting nomenclatural history, as the name combines a non-fossil epithet with a fossil taxon at the generic rank (therefore, the dagger preceding †*Lingulodinium* D.Wall). This results from the abundant practice in dinophyte taxonomy to describe motile cells as non-fossils and coccoid cells as fossils (although there is no necessary link between stage of life-history and stratigraphy). Initially identified as a motile and thecate dinophyte (Stein 1883), coccoid cells (or frequently 'cysts' in the literature) were assigned to non-fossil *L. polyedra* early (Nordli 1951, who treated the species under *Gonyaulax* Diesing). Later, Wall and Dale (1967) identified similar extant such cells as the fossil †*Lingulodinium machaerophorum* (Deflandre & Cookson) D.Wall. It was then Dodge (1989), who also formally included *L. polyedra* in †*Lingulodinium*, which still requires substantial taxonomic revision of its constituent species (both non-fossil and fossil: Wall et al., 1973; Head et al., 1994).

Like almost all microalgae described before the dawn of DNA sequencing, the taxonomic identity of *L. polyedra* remains ambiguous. This is also illustrated by divergent sequences deposited in GenBank under the same scientific name, and it is unclear which entries refer to the true *L. polyedra*. The names of several dinophytes have been clarified in the past years based on a powerful tool provided by the *International Code of Nomenclature for algae, fungi, and plants* (ICN: Turland et al., 2018), namely the epitypification approach (Kretschmann et al., 2018). Some already epitypified taxa have been described from Kiel Fjord

* Corresponding author.
E-mail address: gottschling@bio.lmu.de (M. Gottschling).

https://doi.org/10.1016/j.hal.2020.101956
Received 5 June 2020; Received in revised form 26 November 2020; Accepted 26 November 2020
Available online 4 March 2021

(Zinßmeister et al., 2011; Kretschmann et al., 2015; Tillmann et al., 2017, 2019).

Gonyaulacales are a prime component of the thecate Dinophyceae and comprise some 350 extant species. Habitat preference is clearly marine (Gómez, 2012b), but the group includes also freshwater algae such as *Ceratium* Schrank and *Gonyaulax clevei* Ostenf. (Moestrup and Calado, 2018). A number of gonyaulacalean dinophytes have gained questionable fame, because they are producers of various potent toxins (Holmes et al., 2014; Rhodes and Wood, 2014). Best known examples are some species of *Alexandrium* Halim that produce saxitoxins, being potent neurotoxins responsible for paralytic shellfish poisoning, but other species of *Alexandrium* produce also spirolides, goniodomines, gymnodimines and/or poorly characterised lytic compounds (Anderson et al., 2012). Species of *Fukuyoa* F.Gómez, D.J.Qiu, R.M.Lopes & Senjie Lin and *Gambierdiscus* Adachi & Fukuyo are producers of Ciguatera toxins including maitotoxin, which is regarded as the most toxic compound in marine habitats (Parsons et al., 2012; Soliño and Costa, 2018). Further Gonyaulacales produce palyand ovatoxins (*Ostreopsis* E.J.Schmidt: Parsons et al., 2012) or yessotoxins (†*Lingulodinium, Protoceratium* Bergh, some species of *Gonyaulax*: Tubaro et al., 2010).

The classification of Fensome et al. (1993, continuously updated in Williams et al., 2017) integrates non-fossil and fossil dinophytes and aims at systematics reflecting the phylogeny of the group. Three types of hypothecal plate arrangements are readily distinguished in Gonyaulacales, namely the sexiform, quinqueform and partiform patterns, corresponding to gonyaulacoid, pyrocystoid (previously goniodomatoid, but corresponding names have been rejected at generic and family ranks: Elbrächter and Gottschling, 2015; Gottschling and Elbrächter, 2015; Prud'homme van Reine, 2017) and cladopyxidoid dinophytes. No DNA sequence information is available from the latter group at present, or taxa with a partiform hypotheca such as Amphidomataceae show only distant relationships to Gonyaulacales (Tillmann et al., 2012; Gottschling et al., 2020). For this reason, cladopyxidoid dinophytes and the partiform configuration are not further considered here. The quinqueform differs from the sexiform configuration (Fig. 2) in the shape of the second antapical plate (or Y plate in Taylor-Evitt notation: Taylor, 1980, 1990; Evitt, 1985; Fensome et al., 1993) and in the lack of its contact to the sixth postcingular plate (plate VI in Taylor-Evitt notation).

In molecular phylogenetics, Gonyaulacales were early recognised as monophyletic (Daugbjerg et al., 2000; Saldarriaga et al., 2001), which was confirmed by subsequent analyses using concatenated DNA sequences and a reasonably broad taxon sample (Orr et al., 2012; Tillmann et al., 2012; Gu et al., 2013; Gottschling et al., 2020). The uniqueness of the group is also morphologically expressed by an increased asymmetrical arrangement of thecal plates and particularly by the lack of contact between the plate sp (Z plate in Taylor-Evitt notation) and the first postcingular homologue (Iu plate in Taylor-Evitt notation). This contact is only present in cladopyxidoid dinophytes but not in the core group of Gonyaulacales (Fensome et al., 1993).

In this study, the taxonomic identity of *L. polyedra* is clarified based on material collected at the type locality. The DNA sequences gained are embedded in a molecular phylogeny of Gonyaulacales as inferred from concatenated sequences of the ribosomal RNA (rRNA) operon. The principal subdivision of core Gonyaulacales into the two entities of quinqueform and sexiform hypothecal arrangement is tested using molecular phylogenetics, hypothesising a sister group relationship between the two groups. The taxon sample has been compiled from a curated voucher list and aims to include as many sequences as possible that have been gained from type material or equivalents thereof. The phylogenetic tree may serve as basis for an improved classification of the Gonyaulacales in future.

2. Materials and methods

2.1. Sampling, cell isolation, cultivation

A surface water sample (temperature: 15.5 °C, salinity: 17.5) and a phytoplankton net tow sample (20 μm mesh size) was taken at Kiel Fjord (Germany) from a pier at 54°19.87 N and 10°9.04 E on 9th September 2019 (Tab. S1). Single cells were isolated by micro-capillary pipets into 96-well plates filled with 0.2 mL filtered water from the sample site. Plates were incubated at 15 °C under a photon flux density of 80 μmol m^{-2} s^{-1} on a 16:8 h light:dark photocycle in a controlled environment growth chamber (Sanyo Biomedica MIR 252; Wood Dale, USA–IL). A total of three clonal strains of *L. polyedra* (K3-G2, K3-G5, K3-G8) were established and subsequently grown at the culture conditions described above in an natural seawater medium consisting of sterile filtered (0.2 μm VacuCap filters; Pall Life Sciences; Dreieich, Germany) and diluted North Sea water with a salinity of about 15, containing nutrients corresponding to 50% of K-medium (Keller et al., 1987) slightly modified by omitting addition of ammonium ions.

For DNA harvest, cells were collected by centrifugation (Eppendorf 5810R; Hamburg, Germany) in 50 mL centrifugation tubes at 3220 × *g* for 10 min. Cell pellets were transferred with 0.5 mL lysis buffer (SL1, provided by the NucleoSpin Soil DNA extraction Kit; Macherey-Nagel; Düren, Germany) to 1 mL microtubes and stored frozen (–20 °C) for

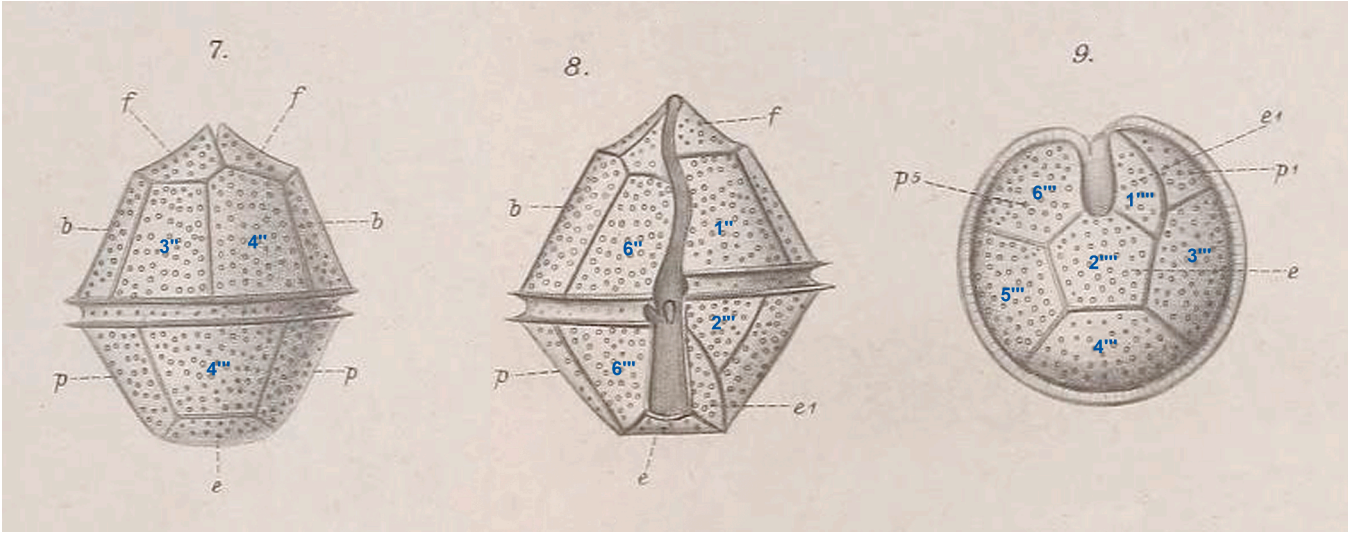

Fig. 1. Friedrich v. Stein's original material of *Lingulodinium* (≡ *Gonyaulax*) *polyedra* (reproduction of pl. IV 7–9, complemented with Kofoidean plate labels in our interpretation). Note that pl. IV 8 is chosen as lectotype.

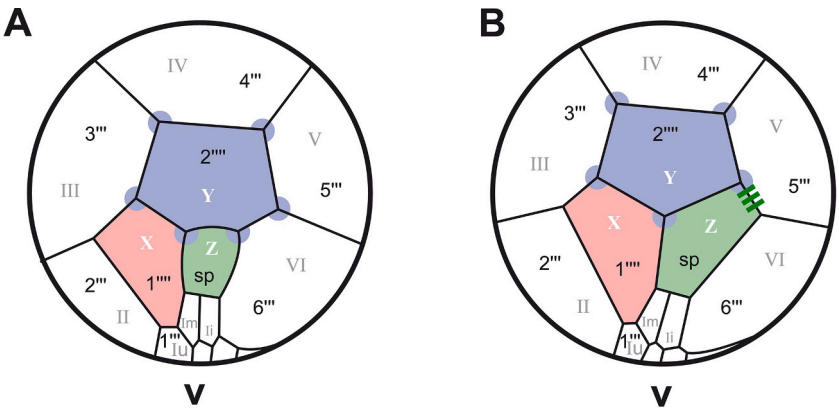

Fig. 2. Comparative sketches of sexiform (A) and quinqueform (B) configurations of the hypotheca found in core Gonyaulacales ('v' indicates the ventral side of the cell). For plate labelling, we follow the Kofoidean notation in black colouring, while the Taylor-Evitt notation is in grey. Note the different shapes of the second antapical plate and the (absent or established) connection between the posterior sulcal plate and the fifth postcingular plate.

subsequent DNA extraction. In addition, all strains of *L. polyedra* were grown in 300 mL plastic culture flasks and harvested as described above for yessotoxins (YTXs) and paralytic shellfish poisoning toxins (PSTs) analysis and stored at –20 °C until use. For each harvest, cell density was determined by settling Lugol-fixed samples and counting >400 cells under an inverted microscope.

2.2. Microscopy

Observation of living or fixed cells (formaldehyde: 1% final concentration, or neutral Lugol-fixed: 1% final concentration) was carried out using an inverted microscope (Axiovert 200 M; Zeiss; Munich, Germany) and a compound microscope (Axiovert 2; Zeiss), both equipped with epifluorescence and differential interference contrast optics. Light microscopic examination of thecal plates of *L. polyedra* was performed on fixed cells (neutral Lugol) stained with Solophenyl Flavine 7GFE500, a fluorescent dye specific to cellulose (Chomérat et al., 2017). Epifluorescence microscopy was used to observe chloroplasts (filter set 09; Zeiss) and to determine the shape and location of the nucleus (UV excitation, filter set 01; Zeiss) after staining of formalin-fixed cells with 4′,6-diamidino-2-phenylindole (DAPI, 0.1 μg mL^{-1} final concentration) for 10 min. Images were taken with a digital camera (Axiocam MRc5; Zeiss). Cell length and width were measured at 1000x microscopic magnification using freshly fixed cells (Lugol, 1% final concentration) from dense but healthy and growing strains (based on stereomicroscopic inspection of the living material) at late exponential phase and the Axiovision software (Zeiss).

For scanning electron microscope (SEM) observations, cells of *L. polyedra* were collected by centrifugation (Eppendorf 5810R; 3220 × *g* for 10 min) from 10 to 50 mL of the strain, depending on cell density. The supernatant was removed, and the cell pellet re-suspended in 60% ethanol prepared in seawater (final salinity ca 13) in a 2 mL microtube at 4 °C for 1 h in order to strip off the outer cell membrane. After centrifugation and removal of the diluted seawater supernatant, cells were fixed with formaldehyde (2% final concentration in a 60:40 mixture of deionised water and seawater) and stored at 4 °C for 3 h. Alternatively, cells were treated with TritonX (Sigma-Aldrich; St Louis, USA–MO) at 0.2–0.5% final concentration for 1–3 h. Cells from both pre-treatment methods were collected and processed for SEM (FEI Quanta FEG 200; Eindhoven, the Netherlands) as described in Tillmann et al. (2019).

2.3. Toxin analysis

For YTXs analysis, cell pellets were suspended in 500 μL methanol and subsequently transferred to a FastPrep tube containing 0.3 mL of lysing matrix D bulk beads (MP biomedicals; Eschwege, Germany). The samples were homogenised by reciprocal shaking in a Bio101 FastPrep instrument (Thermo Savant) at maximum speed (6.5 m s^{-1}) for 45 s. After homogenisation, samples were centrifuged (Eppendorf 5415 R) at 16,100 × *g* at 4 °C for 15 min. Supernatants were transferred to spin-filters (pore-size 0.45 μm; Millipore; Eschborn, Germany) and centrifuged at 800 × *g* at 10 °C for 30 s. Filtrates were transferred into 2 mL autosampler glass vials and placed under a continuous stream of N_2 until complete dryness. These residues were then dissolved in 100 μL MeOH. All extracts were stored at –20 °C until analysis. Toxin analysis was performed on a liquid chromatograph (LC1100 series, Agilent; Waldbronn, Germany) coupled to a triple quadrupole mass spectrometer (API 4000 QTrap, Sciex; Darmstadt, Germany) with turbo-spray ionisation in the negative mode following the methods in Sala-Pérez et al. (2016) and Peter et al. (2018). Yessotoxins were detected in the selected reaction monitoring mode with mass transitions given in Sala-Pérez et al. (2016) and Peter et al. (2018). Toxin contents were determined by calibration against an external standard of yessotoxin (YTX) (CRM, IMB-NRC; Halifax, Canada) and all YTX variants other than YTX were expressed as YTX equivalents.

For PST analysis, cell pellets were extracted with 500 μL of 0.03 M acetic acid and homogenised as described above. Supernatants were transferred to spin filters (0.45 μm pore size, Millipore) and centrifuged at 800 × *g* for 30 s, followed by transfer to autosampler vials. Toxins were analysed by ion-pair chromatography coupled with postcolumn derivatisation and fluorescence detection (PCOX method) as described in detail by Van de Waal et al. (2015).

2.4. DNA extraction, sequencing and molecular phylogenetics

Genomic DNA was extracted following the manufacturers' instructions of the NucleoSpin Soil DNA extraction Kit (Macherey-Nagel) with an additional cell disruption step within the beat tubes; the samples were shaken for 45 s and another 30 s at a speed of 4.0 m s^{-1} in a FastPrep FP120 cell disrupter (Thermo Savant; Illkirch, France). For the elution step, 50 μL of the provided elution buffer were spun through the spin column, and elution was subsequently repeated with another 50 μL to increase the DNA yield, leading to a total elution volume of 100 μL. Various regions of rRNA genes, including the small (SSU) and large (LSU) subunit and the Internal Transcribed Spacers (ITSs), were amplified using the following primer sets: 1F (5′−AAC CTG GTT GAT CCT GCC AGT−3′) and 1528R (5′−TGA TCC TTC TGC AGG TTC ACC TAC−3′) for the SSU; ITS1 (5′−TCC GTA GGT GAA CCT GCG G − 3′) and ITS4 (5′−TCC GCT TAT TGA TAT GC−3′) for ITS; DirF (5′−ACC CGC TGA ATT TAA GCA TA−3′) and D2CR (5′−CCT TGG TCC GTG TTT CAA GA−3′) for LSU. Conditions of the PCR for the respective region, amplicon check and purification, as well as the sequencing process,

followed the protocols described in Tillmann et al. (2020) and Wietkamp et al. (2019).

Full voucher information of the systematically representative set comprising 316 gonyaulacalean dinophytes (plus 13 outgroup accessions) are provided in Table S1. It is aimed to display the currently known molecular diversity of gonyaulacalean dinophytes and in case of identical or highly similar sequences deposited in GenBank, those accessions were chosen, of which the longest rRNA (if applicable concatenated) sequences were available. Furthermore, it is aimed to consider as many sequences being equivalent to type material as possible and to include all GenBank entries assigned to †*Lingulodinium*. There is only little similarity between *Grammatodinium* Zhun Li & H.H. Shin and thecate dinophytes, and its assignment to the Gonyaulacales based on molecular phylogenetics (Li et al., 2017; Gottschling et al.,

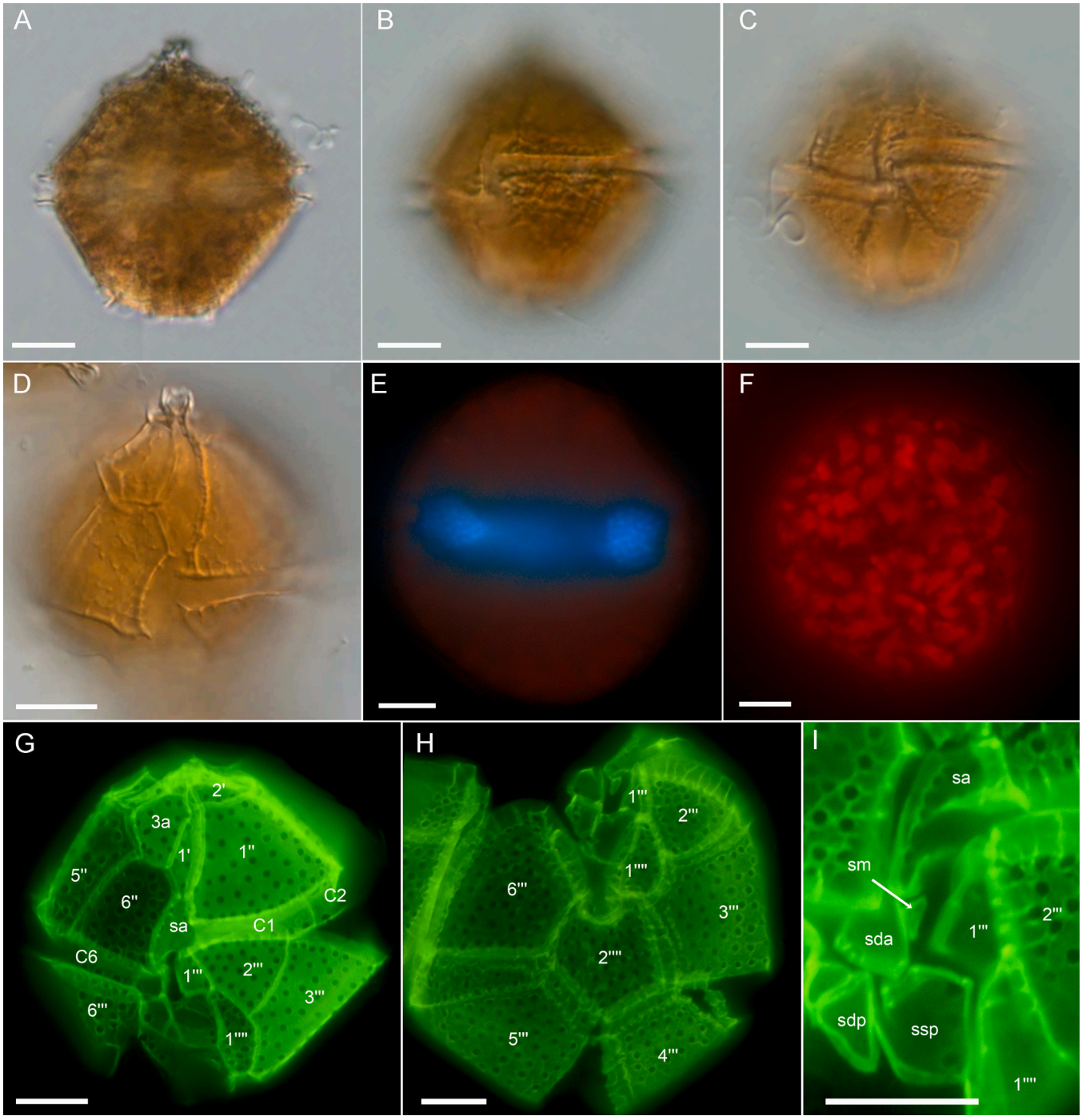

Fig. 3. *Lingulodinium polyedra* (strain K3-G8), light microscopy of living cells (A–C) or formaldehyde fixed cells (D–I). (A–C) Cells in ventral view in mid-cell focus (A), in slightly right-lateral view (B) or with focus on the cingulum (C). (D) Apical ventral view, note the raised apical pore complex and shape of the first apical plate. (E) Cell stained with DAPI and viewed with epifluorescence and UV excitation. (F) Cell in epifluorescence and blue light excitation to illustrate chloroplasts shape and distribution. (G–I) Different thecae stained with Solophenyl Flavine and viewed with epifluorescence and green light excitation; note that younger were lighter than older plates and that the pores on the younger plates had no rim. (I) Detailed view of the sulcal area. Plate labels according to the Kofoidean system. Sulcal plate labels: sdp = right posterior sulcal plate; ssp = left posterior sulcal plate; sda = right anterior sulcal plate; sm = median sulcal plate; sa = anterior sulcal plate. Scale bars = 10 μm.

2020) could rely on long branch attraction (Bergsten, 2005). However, inclusion or exclusion of *Grammatodinium* in the DNA sequence data set significantly changed neither topology nor statistical assessment of the molecular trees, that they were included in the present analyses. For alignment constitution, separate matrices of the rRNA operon (i.e., SSU, ITS, LSU) were constructed, aligned using 'MAFFT' v6.502a (Katoh and Standley, 2013) and concatenated afterwards. The aligned matrix is available as *.nex file upon request.

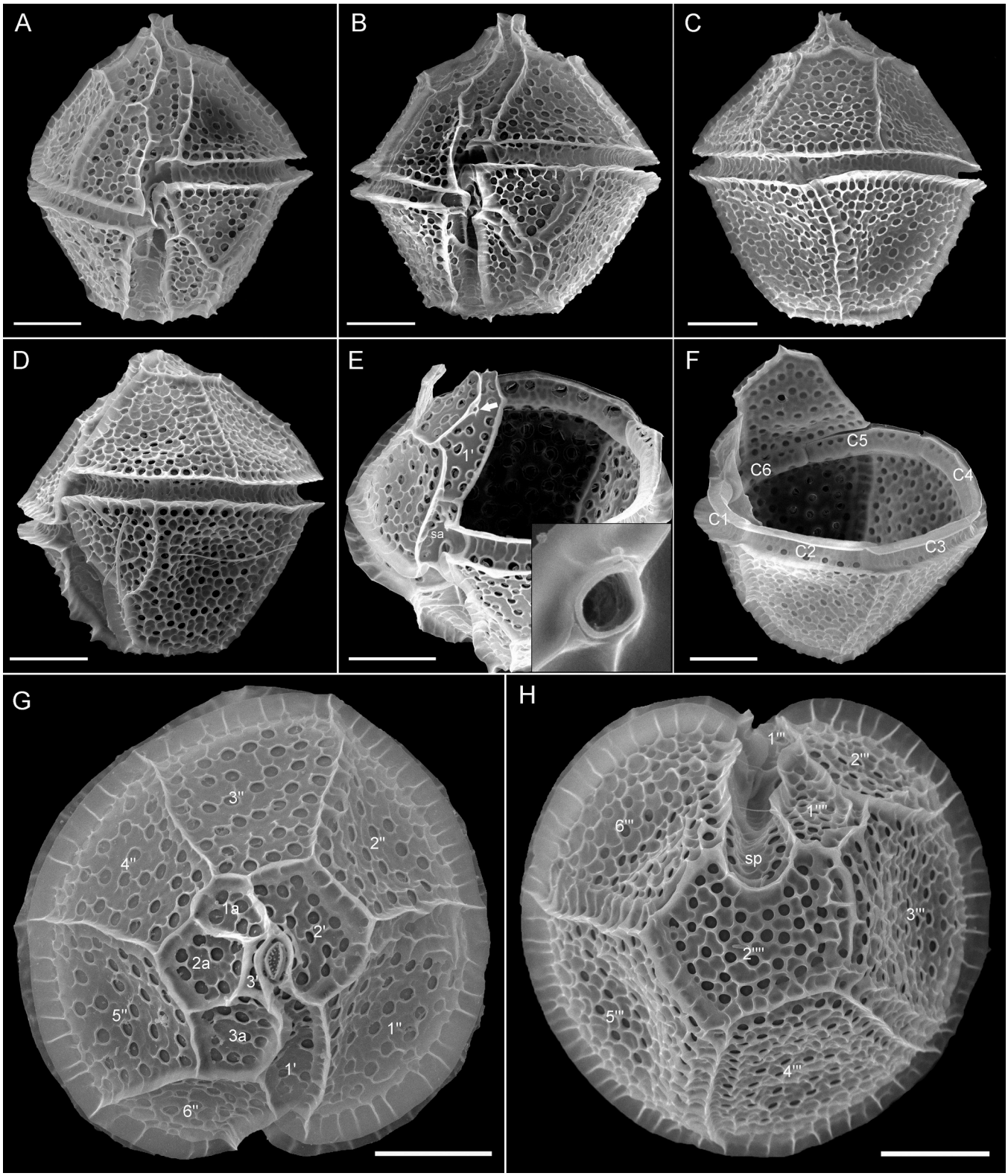

Fig. 4. *Lingulodinium polyedra* (strain K3-G8), SEM of different cells in ventral view (A, B), dorsal view (C) or left-lateral view (D). (E) Location and structure of the ventral pore (white arrow, enlarged view in the figure insert). (F) Internal view of cingular plates. (G) Epithecal plates in apical view. (H) Hypothecal plates in antapical view. Scale bars = 10 μm.

Phylogenetic analyses were carried out using Maximum Likelihood (ML) and Bayesian approaches, as described in detail previously (Gottschling et al., 2012, 2020) using the resources available from the CIPRES Science Gateway (Miller et al., 2010). The Bayesian analysis was performed using 'MrBayes' v3.2.6 (Ronquist et al., 2012, freely available at http://mrbayes.sourceforge.net/download.php) under the GTR+Γ substitution model and the random-addition-sequence method with 10 replicates. Two independent analyses of four chains (one cold and three heated) were run with 20,000,000 generations, sampled every 1,000th cycle, with an appropriate burn-in (10%) as inferred from the evaluation of the trace files using Tracer v1.5 (http://tree.bio.ed.ac.uk/software/tracer/). For the ML calculation, the MPI version of 'RAxML' v8.2.4 (Stamatakis, 2014, freely available at http://www.exelixislab.org/) was applied using the GTR+Γ substitution model under the CAT approximation. The best-scoring ML tree was determined, and 1,000 non-parametric bootstrap replicates (rapid analysis) were performed in a single step. Statistical support values (LBS: ML bootstrap support, BPP: Bayesian posterior probabilities) were drawn on the resulting, best-scoring tree.

3. Results

3.1. General morphology of Lingulodinium polyedra

All three clonal strains of *L. polyedra* were morphologically identical. Strain K3-G8 was selected for the preparation of the epitype (see below) and is described and depicted in detail (Figs 3–6). Cell size for all strains ranged from 37.6 to 52.5 μm in length and 33.8 to 47.9 μm in width (Table 1). Mean size of strain K3-G8 was 45.0 μm in length and 42.8 μm in width. Based on observations of swimming cells, there was no dorso-ventral compression. Cells divided by desmochisis. Newly divided cells were identifiable by different degrees of ornamentation in maternal and new plates (Figs 3G, S5). The division line thereby determined, along

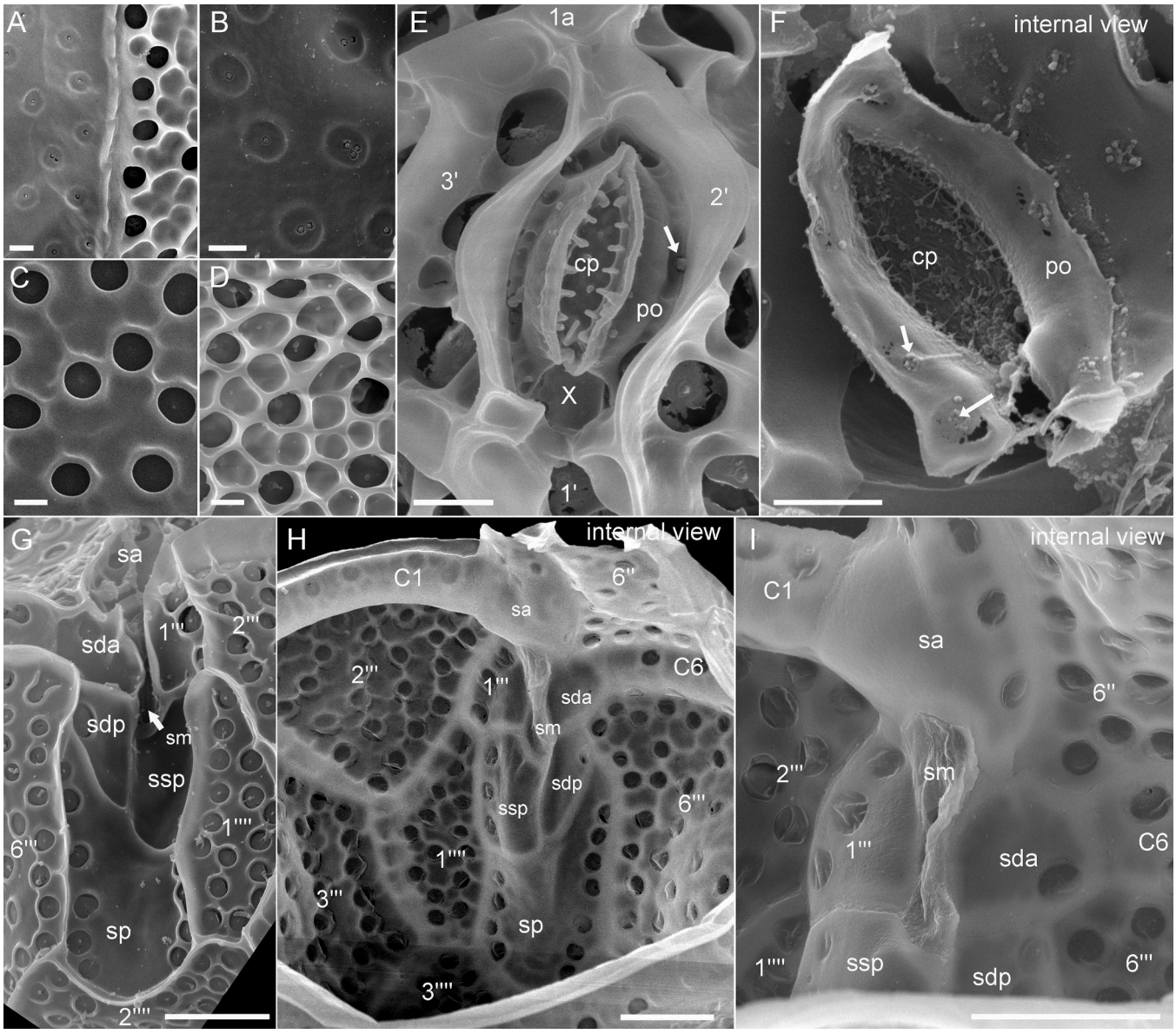

Fig. 5. *Lingulodinium polyedra* (strain K3-G8), details of thecal plate structure and arrangement. (A–D) Plate surface ornamentation. (A) Plate suture of a recently divided cell; left side thin and faintly structured. (B) Detailed view of a faintly structured young plate showing one to three small trichocyst pores in the ring centre. (C–D) Two different stages of increasing ring ornamentation. (E–F) Detailed view of the apical pore complex. Note the presence of a small X-plate and the presence of pores (white arrows in E–F) on the pore plate. (F) Pore plate in internal view. (G–I) Sulcal plate arrangement in external (G) and internal (H–I) views. Plate labels according to Kofoidean system. cp = cover plate; po = pore plate; X = X-plate; sp = posterior sulcal plate; sdp = right posterior sulcal plate; ssp = left posterior sulcal plate; sda = right anterior sulcal plate; sm = median sulcal plate; sa = anterior sulcal plate. Scale bars = 1 μm (A–F) or 5 μm (G–I).

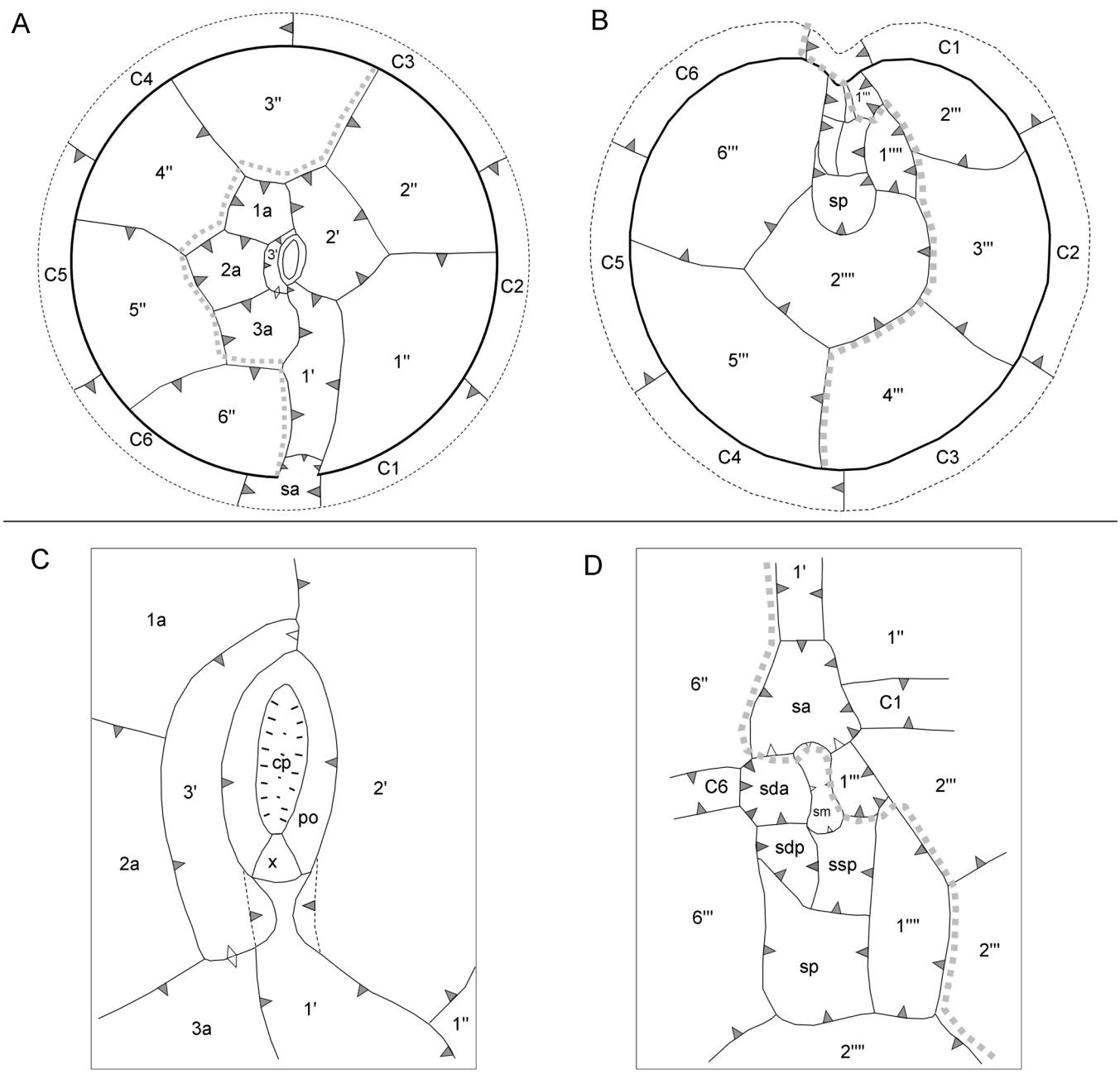

Fig. 6. Schematic line drawings of *Lingulodinium polyedra* plate pattern, plate overlap and division line. (A) Epithecal plates in apical view. (B) Hypothecal plates in antapical view. (C) Apical pore complex and apical plates. (D) Central ventral area and sulcal plates. Arrows indicate plate overlap, with white arrows indicating that overlap direction for that particular suture could not been identified with certainty. Wide grey dotted line: cell division line along which plates are separated during cell division.

Table 1
strain size.

strain	length (μm) **mean** ± SD min-max	width (μm) **mean** ± SD min-max	l/w ratio **mean** ± SD min-max	N
K3-G2	**46.1** ± 2.7 39.4–52.5	**42.8** ± 2.5 37.8–47.6	**1.08** ± 0.04 1.00–1.18	50
K3-G5	**44.5** ± 2.8 37.6–51.1	**41.4** ± 3.0 33.8–47.9	**1.08** ± 0.04 0.98–1.16	50
K3-G8	**45.0** ± 1.5 42.1–47.7	**42.8** ± 2.3 38.1–47.5	**1.05** ± 0.03 1.00–1.15	50

which the maternal plates separated and being distributed to the daughter cells, is marked in Fig. 6. The large nucleus (Fig. 3E) had the shape of a hemi-torus and was located in the cingular plane, with both ends faintly visible in ventral focus of LM. The cells were brown-orange in colour (Fig. 3A–D) with numerous small chloroplasts scattered throughout the cell (Fig. 3F).

The cells' outlines were heptagonal in ventral or dorsal view. The two obtuse angles of the in outline pentagonal epitheca resulted from the boundary between the precingular and apical plate series (Figs 3A, 4A–D). The epitheca had a small, raised apical pore complex (APC; Figs 3A, 4A–D). The hypotheca was trapezoidal in outline with straight lines and a flat antapex without projections (Fig. 4B–D). In polar view, cells were nearly circular in outline (Fig. 4G–H). The cingulum was almost median, narrow (8–9% of cell length), incised and exhibited narrow

cingular lists, which were ca 2.2 μm (range 1.8–2.8 μm, $n = 20$) in width (Figs 3–4). The cingulum was descending and displaced without overhang for ca two cingular widths (Figs 3C, 4A–B, D).

The plate formula was APC (Po, X, cp), 3′, 3a, 6″, 6c, 6s, 6‴, 2⁗ and is schematically shown in Fig. 6. The epitheca comprised of six precingular plates, the APC and six climactal plates (Fig. 4G). Of these, three plates were in direct contact to the pore plate fulfilling the definition of apical plates. The ventrally located plate 1′ was narrow, irregular in shape and ranged from the anterior sulcal plate to the pore plate. Plate 2′ on the left-lateral side was heptagonal and large. Apical plate 3′ right of the pore plate was small and hexagonal. On the cells' right side, there were three anterior intercalary plates, which were all pentagonal and approximately of the same size.

Within the APC, there was an elongated oval pore plate (Fig. 5E), which had a few pores (Figs 5E–F, S1C, K–L) and which was bordered by a raised rim formed by the adjacent apical plates 2′ and 3′. Ventrally, the pore plate abutted the first apical plate, which was difficult to observe, because the rim of plates 2′ and 3′ tended to overgrow plate 1′ in its anterior part (Fig. S1). In the centre of the pore plate, there was a narrow tube with an oval outline and terminated by a cover plate, which was flecked by small, elongate structures. Ventrally, the pore plate had a more or less triangular notch, where a small X-plate was located (Fig. 5E). This X-plate abutted plate 1′ and continued from the base of the pore plate all along the rise of the apical pore to the cover plate (Fig. S1).

If the contact of precingular plates to the cingulum was considered a single side (i.e., irrespective whether one or two cingular plates were contacted), then plates 1″, 3″, 4″ and 5″ were pentagonal, whereas the left-lateral plate 2″ was tetragonal. The precingular plate 6″ was in contact with the sulcal plate sda (Fig. 5G–I) and was thus hexagonal. A ventral pore was present at the right margin of plate 1′, approximately in the middle of the suture between plates 1′ and 3a (Fig. 4E). The pore seemed to be always present, even if it was difficult to detect when, for example, out of focus (Fig. 3D) or when partly hidden by the overlapping plate margin of plate 3a (Fig. S2). This ventral pore was made by a plate-like tube located in a circular notch of plate 1′ (Fig. S2). The mean diameter of the tube was 0.71±0.08 μm (0.58–0.84 μm, $n = 10$).

There were six cingular plates all being of almost the same size (Fig. 4F). The sulcus was a narrow and incised concave groove bordered by sulcal lists, which widened posteriorly and reached the antapex (Figs 4A–B, 5G). Its anterior part was mostly hidden due to a close rank of plate 1‴ on the left and plate sda on the right (Fig. 5G). With its anterior part, plate sa slightly invaded the epitheca. Plate sp had contact neither to the first nor to the fifth postcingular plate (see also Fig. 2). There was a central area in the anterior part of the sulcus commonly termed 'flagellar pore'. In fact (and most obvious from internal view: Fig. 5H–I), it was an internal vaulted cavity made of at least one if not two plate-like structures being in contact with plates sa, sda, 1‴, sdp and ssp. Slightly disintegrated cells (observed with fluorescence-microscopy of cellulose-stained cells) revealed the presence of at least one small central platelet regarded here as a median sulcal plate sm (Fig. 3I). With the exception of the central, tiny plate sm, sulcal plates were at least partly ornamented and porate (Fig. 5G–I). In plates ssp, sdp and sda, pores were low in number.

On the hypotheca, there were six postcingular and two antapical plates (Fig. 4H). The anterior left-lateral part of the sulcal groove was formed by plate 1‴ having a kink to plate 2‴. The first postcingular plate 1‴ was small and irregular in shape. Plate 2‴ was triangular and notably smaller than the remaining large postcingular plates 3‴–6‴. Postcingular plate 3‴ was pentagonal and plates 4‴ through 6‴ tetragonal, whereas the terminal plate 6‴ had contact to three sulcal plates (Figs 5H, 6B). Plate 2⁗ was in antapical position and hexagonal ('sexiform', see also Fig. 2A), with one side deeply concave resulting from the sulcal groove. Antapical plate 1⁗ was ventrally located on the left side of the sulcus, and its shape was irregularly polygonal and elongate (Figs 3H, 4A).

The surface of mature thecal plates was coarsely areolate with multiple round structures (diameter: 0.94–1.33 μm, $n = 10$) interconnected by ridges (Fig. 4). In young daughter cells, these rings were visible as faint risings (Fig. 5A–B) with one, two or three small pores (diameter of the small pores: ca 160–200 nm, $n = 10$) in the centre (Fig. 5B). Probably with plate age, elevated structures around the rings were formed (Fig. 5C) and were increasingly connected by ridges. At a later stage, plate ornamentation of areas between the rings may form a reticulum resembling an irregular honeycomb (Fig. 5D).

On the theca, there were distinct ridges along the plate sutures (Fig. 4). On the side of the ridges, there were growth rims of varying width, especially well developed in the adcingular plates (Fig. S3). Ridges and rims were arranged accordingly to the plate overlap pattern, with a growth rim overlapping the adjacent plate. The corresponding plate overlap scheme is illustrated in Fig. 6. Keystone plates (i.e., those which overlap all adjacent plates) were 3″, C3 and 4‴ in the precingular, cingular and postcingular series, respectively. Precingular and cingular plates had broad and planar abutting areas (Fig. S3), whereas the contacts between postcingular and cingular plates could not be documented unambiguously. For apical plates and all small plates in the sulcal area, overlap was difficult (Fig. 5I) if not impossible to observe. Subsequently, plate sutures between apical plates 2′ and 3′, between plates sa and sda or 1‴ and between the plates adjacent to the central sulcal plate sm could not be determined reliably (indicated by white arrows in Fig. 6).

3.2. Phycotoxins

For none of the *L. polyedra* strains established in the present study, yessotoxin (YTX *m/z* 1141) could be detected, but all three strains contained homo-YTX (*m/z* 1155; Table 2). Homo-YTX was the only YTX congener in two of the strains, and one strain additionally contained a hydroxy-YTX variant (*m/z* 1157). Cell quotas of total YTXs ranged from 23 to 76 fg cell^{-1} (Table 2). The detection limit of YTX and its variants ranged between 3.3 (strain K3-G8) and 17 fg cell^{-1} (strain K3-G2) depending on available biomass. None of the strains contained PSP toxins above LOD (< 0.1 pg cell^{-1}, for each PSP compound listed in Tab. S2).

3.3. Molecular phylogenetics

The SSU+ITS+LSU alignment was 1,983+726+3,622 bp long and comprised 1,005+642+1,897 parsimony-informative sites (56.0%, mean of 10.8 per terminal taxon) and 4,882 distinct RAxML alignment patterns, respectively. Figures 7–8 and S6 show the best DNA tree (in three parts), and topologies were largely congruent regardless of whether ML or Bayes' theorem was applied. The Gonyaulacales were monophyletic (84LBS, .98BPP) and segregated into seven lineages at high taxonomic level (Fig. 7): †Lingulodiniaceae Sarjeant & C.Downie (100LBS, 1.00BPP), Thecadiniaceae Balech (85LBS, 1.00BPP), Ceratocorythaceae Er.Lindem. (= Protoceratiaceae Er.Lindem.; 88LBS, 1.00BPP), Gonyaulacaceae Er.Lindem. (100LBS, 1.00BPP), Ceratiaceae Er.Lindem. (99LBS, 1.00BPP), †*Dapsilidinium* J.P.Bujak, C.Downie, G.L. Eaton & G.L.Williams+*Grammatodinium* (76LBS, 1.00BPP) and Pyrocystaceae Apstein (81LBS, 1.00BPP). The relationships between such lineages was not ultimately resolved, but †Lingulodiniaceae appeared as sister group of all other Gonyaulacales (90LBS, 1.00BPP).

Table 2
Results YTX contents analysis (cell quota as fg cell^{-1}).

strain	10^6 cells per pellet	*m/z* 1141 YTX	*m/z* 1155 homo-YTX	*m/z* 1157 OH-YTX
K3-G2	1.22	nd	38.5	37.3
K3-G5	5.23	nd	56.4	nd
K3-G8	6.47	nd	22.8	nd

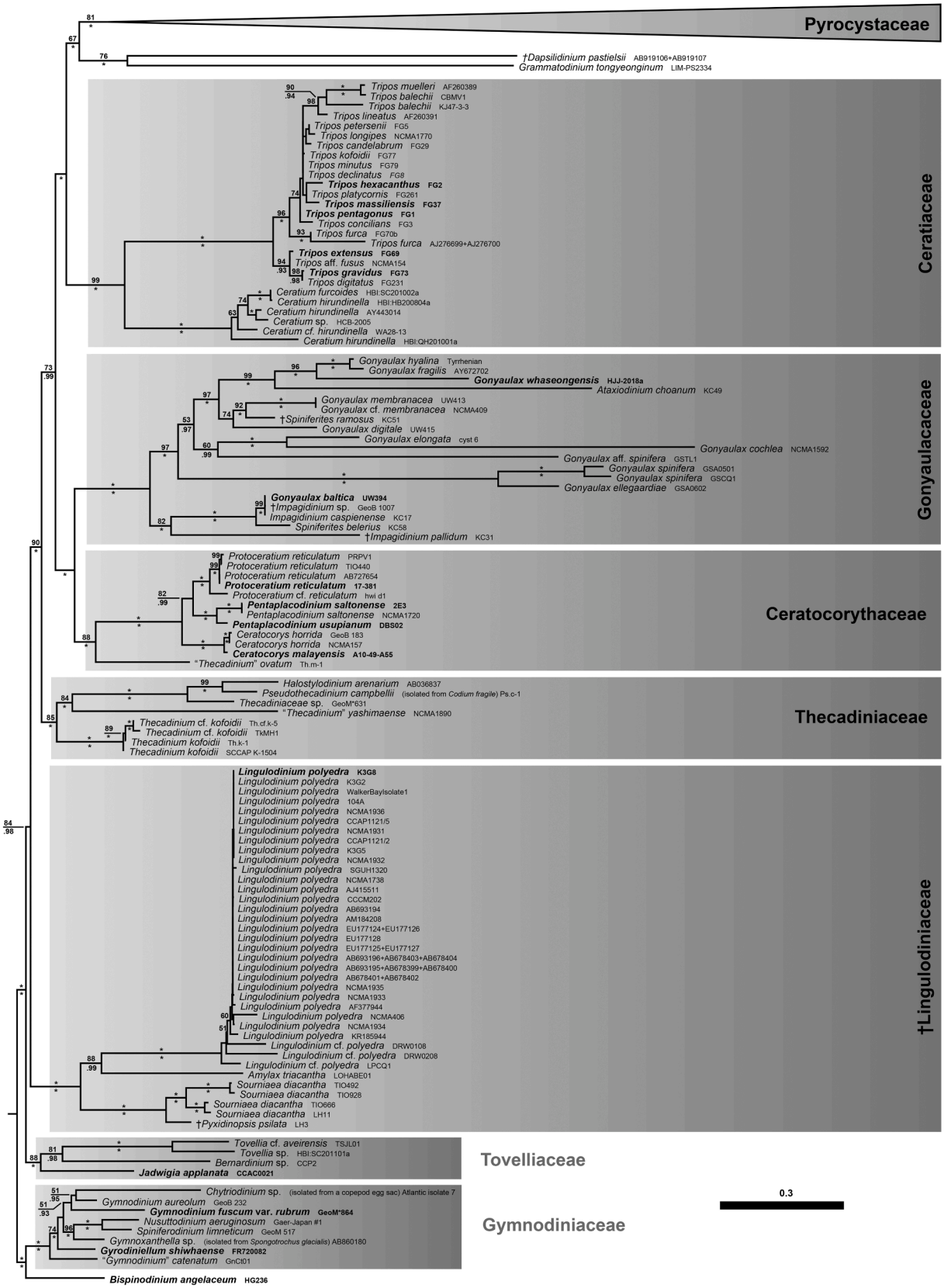

Fig. 7. A molecular reference tree of Gonyaulacales, recognising seven major lineages. Maximum Likelihood tree (–187,475.25) of 316 systematically representative gonyaulacalean sequences (with strain number information and partly collapsed) as inferred from a rRNA nucleotide alignment (3,544 parsimony-informative sites). Numbers on branches are ML bootstrap (above) and Bayesian support values (below) for the clusters (asterisks indicate maximal support values, values under 50 and 0.90, respectively, are not shown).

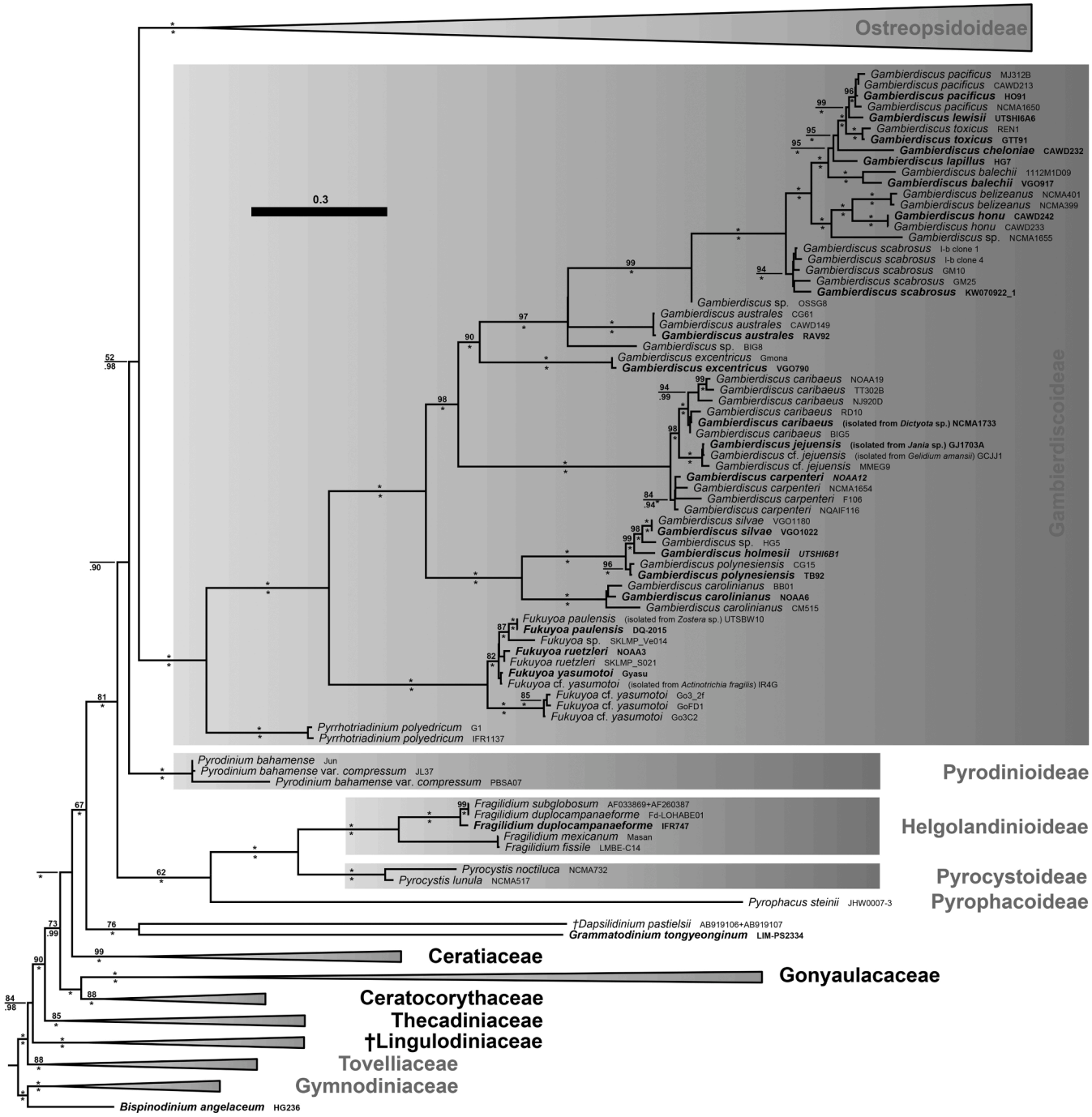

Fig. 8. A molecular reference tree of Pyrocystaceae as part of Gonyaulacales, recognising six major lineages. Maximum Likelihood tree (–187,475.25) of 316 systematically representative gonyaulacalean sequences (with strain number information and partly collapsed) as inferred from a rRNA nucleotide alignment (3,544 parsimony-informative sites). Numbers on branches are ML bootstrap (above) and Bayesian support values (below) for the clusters (asterisks indicate maximal support values, values under 50 and 0.90, respectively, are not shown).

Pyrocystaceae (Fig. 8) segregated into Pyrophacoideae, stat. nov. (single accession), Pyrocystoideae, stat. nov. (100LBS, 1.00BPP), Helgolandinioideae Fensome, F.J.R.Taylor, G.Norris, Sarjeant, Wharton & G.L.Williams (100LBS, 1.00BPP), Pyrodinioideae Fensome, F.J.R.Taylor, G.Norris, Sarjeant, Wharton & G.L.Williams (100LBS, 1.00BPP), Gambierdiscoideae Fensome, F.J.R.Taylor, G.Norris, Sarjeant, Wharton & G.L.Williams (100LBS, 1.00BPP) and Ostreopsidoideae, stat. nov. (100LBS, 1.00BPP). The relationships between such lineages was not reliably resolved, but Helgolandinioideae+Pyrocystoideae, stat. nov., appeared closer related (100LBS, 1.00BPP) and constituted the sister group of Pyrophacoideae, stat. nov. (62LBS, 1.00BPP).

Many subordinate clades corresponded to established taxa at generic rank and were highly supported such as (list not complete) *Ceratium* (100LBS, 1.00BPP), *Fragilidium* Balech (100LBS, 1.00BPP), *Gambierdiscus* (100LBS, 1.00BPP), †*Lingulodinium* (100LBS, 1.00BPP; including three strains from the type locality of *L. polyedra*), *Ostreopsis* (100LBS, 1.00BPP) and *Tripos* Bory (100LBS, 1.00BPP). Notably, the monophyly of *Alexandrium* was not demonstrated (also because species assigned to *Centrodinium* Kof. nested therein: Fig. S6). Rather, *Alexandrium* was composed of five clades, one of which appeared closer related to *Coolia* Meunier+*Ostreopsis* (100LBS, 1.00BPP), whereas the other four constituted a monophyletic group (71LBS). *Coolia* was not monophyletic as well, and

Coolia tropicalis M.A.Faust appeared closer related to *Ostreopsis* (83LBS, 1.00BPP). There was taxonomic confusion within Gonyaulacaceae, and neither *Gonyaulax* nor †*Impagidinium* Stover & Evitt nor †*Spiniferites* Mantell constituted monophyletic assemblages using the current applications of their constituent species names.

Sequences gained from organisms determined as *L. polyedra* showed some variation. Notably, strains DRW0108, DRW0208 (both western North Pacific) and LPCQ1 (eastern North Pacific) showed divergence from other sequences including those obtained from the strains collected at the type locality.

4. Discussion

4.1. Taxonomic identity of Lingulodinium polyedra

The clonal strain K3-G8, isolated from the type locality and documented here in detail, corresponds to the original descriptions and drawings of *L. polyedra* (Stein, 1883). Cell shape, thecal plate arrangement and thecal ornamentation cannot be distinguished from F. v. Stein's minute illustrations, although the central epithecal plate (i.e., plate 1′) appears slightly broader in the present material (Fig. 3D) than in the original drawing (Stein, 1883; pl. IV 8). However, this plate can be slightly sunken and overgrown by adjacent precingular plates, creating the impression of a slender shape. Moreover, Stein (1883) did not observe all plates and neglected the smaller plates that are documentable in high resolution LM and SEM. This is not considered as a serious contradiction to the protologue and thus, there is confidence that *L. polyedra* has been recollected after over 130 years at the type locality providing the opportunity to epitypify the name (see below). The recollection corresponds with the repeated documentation of motile and coccoid cells from the Kiel Fjord determined as *L. polyedra* (Nehring, 1994, 1997; Hällfors, 2004). Coccoid cells as integral part of the life-history of *L. polyedra*, unfortunately, have not been produced by the strains established here during the course of the study.

Stein (1883) did not describe a ventral pore, but the structure is difficult to observe (even with high resolution LM and SEM). Kofoid (1911: pl. XIV 32) was first who clearly saw and depicted the ventral pore of *L. polyedra* at exactly the same position (i.e., on the suture between plates 1′ and 3a) as demonstrated here, and such a pore was described and depicted also by Lewis and Hallett (1997). In contrast, several other studies (Dürr and Netzel, 1974; Kobayashi et al., 1981; Balech, 1988; Lewis and Burton, 1988; Faust et al., 2005) did not report from the ventral pore, but Dodge (1989) charted the structure in his drawings (his Fig. 1H–I) at the junction of plates 1′, 3a and 6″ (although a ventral pore is not unambiguously visible and not explicitly mentioned on the microscopic images). This position –if real– would be distinctly more posterior than observed by Kofoid (1911) as well as in the present study. Regarding the existence of a ventral pore in *L. polyedra*, Kim et al. (2005) added more confusion when they stated (without providing micrographs) that such a structure would be 'sometimes present'. In any case, a ventral pore is consistently discernible in material, from which the epitype of *L. polyedra* has been prepared (as well as for both other new strains: K3-G2 and K3-G5; Fig. S2). Seemingly contradictory reports in the literature are thus not interpreted as a reflection of true morphological differences between strains of *L. polyedra* or intraspecific and -strain variability, due to the difficulties of observation.

The tube-like ultrastructure of platelet vp is reminiscent to the ventral pore of Amphidomataceae, which likewise have a platelet-like substructure (Tillmann et al., 2009). Anyhow, Amphidomataceae are phylogenetically rather distantly related to Gonyaulacales (Tillmann et al., 2012; Gottschling et al., 2020). A ventral pore appears abundant in other gonyaulacalean dinophytes (Dodge, 1989; Balech, 1995; Carbonell-Moore 1996; Álvarez et al., 2016; Escalera et al., 2018; Lim et al., 2018; Mertens et al., 2018; Luo et al., 2019), but its details at the utrastructural level have rarely been described or illustrated before. Only a SEM image of *Sourniaea diacantha* (Meunier) H.Gu, K.N.Mert., Zhun Li & H.H.Shin indicates that the small ventral pore (which is located at the junction of plates 1′, 4′ and 2a) has a tube-like internal structure (although not described as such in Zhang et al., 2020: Fig. 27) being similar to the ventral pore of *L. polyedra* as revealed in the present study. For species of *Alexandrium,* available micrographs or drawings (Balech, 1995) indicate that here, the pore is just a hole in or between the ventral epithecal plates. More research is necessary to determine homology between the ventral pores of gonyaulacalean and amphidomatacean dinophytes and its character evolution, with particular attention to the plate-like, tubular appearance shown here for *L. polyedra*.

Within Gonyaulacales, the X-plate is reliably absent from the APC as documented in SEM images of some gonyaulacalean species (Dodge and Hermes, 1981). Therefore, presence/absence of a X-plate is an important morphological trait in order to distinguish Gonyaulacales from Peridiniales (Fensome et al., 1993). The X-plate, however, is a consistent element of the APC in *L. polyedra* (though difficult to observe as well; included in the Graphical Abstract), and its small size may explain that its existence has been largely neglected [a similar structure was shown though not commented for *Pentaplacodinium saltonense* K.N.Mert., Carbonell-Moore, V.Pospelova & Head: Mertens et al., 2018: Fig. 7F, and was identified for *Acanthogonyaulax spinifera* (G.Murray & Whitting) H. W.Graham: Carbonell-Moore and Mertens, 2020: Figs 4, 8]. Species of *Gonyaulax* share an APC very similar to *L. polyedra* [e.g., *G. alaskensis* Kof., *G. digitale* (C.H.G.Pouchet) Kof., *G. reticulata* Kof. & J.R.Michener: Dodge 1989; *G. fragilis* (F.Schütt) Kof.: Escalera et al., 2018; *G. rotundata* Rampi: Dodge 1988; *G. whaseongensis* A.S.Lim, H.J.Jeong & Ji H.Kim: Lim et al., 2018], having an oval shape, a tube-like, marginate pore with an oval outline, overlain by a cover plate, and a raised rime around the pore plate made by the adjacent apical plates. However, more high-resolution SEM studies, particularly of the APC, are necessary to uncover the existence and distribution of a small X-plate in gonyaulacalean dinophytes. Size and position of the X-plate is strikingly similar to Amphidomataceae (Tillmann et al., 2009, 2012) despite the already noted distant relationship to Gonyaulacales. There, the X-plate is also small and centrally located allowing contact of the first apical plate 1′ to the pore plates on both sides of the X-plate. Moreover, the X-plate of *L. polyedra* is in contact with the cover plate, as it is present in Amphidomataceae as well (here, by a finger-like outer extension of the X-plate: Tillmann et al., 2009, 2012). A contact between the X-plate and the cover plate is usually not established in Peridiniales and has only been reported for some species of *Heterocapsa* F.Stein (Tillmann et al., 2017; Sunesen et al., 2020).

Whether sequence variation amongst organisms determined as *L. polyedra* (though frequently without detailed morphological study) result from speciation, or corresponds to intraspecific variability, remains unclear. Other gonyaulacalean dinophytes such as *A. ostenfeldii* (Paulsen) Balech & Tangen in fact show intraspecific sequence variability (Kremp et al., 2014), whereas different species of peridinialean dinophytes such as *Apocalathium* Craveiro, Daugbjerg, Moestrup & Calado cannot be differentiated as inferred from rRNA sequence data (Gottschling et al., 2005; Craveiro et al., 2017).

4.2. The thecal plate pattern in gonyaulacalean dinophytes

Two concurring plate labelling systems have been established in gonyaulacalean dinophytes, namely the Kofoidean system (Kofoid, 1909), which is broadly adopted also for peridinialean dinophytes, and later the Taylor-Evitt notation (Taylor, 1980, 1990; Evitt, 1985; Fensome et al., 1993; Fig. 2). Both approaches claim the consideration of plate homologies as fundamental concept that are, however, still partly unresolved and under continuous discussion. At least, there is broad consensus in the literature about the numbers of epithecal, cingular and hypothecal plates of *L. polyedra*, but homology and labelling of plates subsequently differ amongst authors (Table 3).

In the epitheca, the differences are mainly based on divergent

interpretations of the dorsalmost climactal plate (labelled as E4 in Table 3), which is either regarded as an apical plate or as an anterior intercalary plate, and the interpretation affects the labelling of other epithecal plates. The dorsalmost plate is close to the pore plate in our material, but it is never in contact with it (Fig. 5E, S1) and thus, *L. polyedra* has three apical and three anterior intercalary plates (Balech, 1988; Dodge, 1989; Steidinger and Tangen, 1996). Furthermore, *L. polyedra* has a small plate right of the pore plate (labelled as E3 in Table 3), which is also present in *Gonyaulax*. Unfortunately, this structure has received multiple labels, namely plate Cv in the alternative Taylor-Evitt notation (Fensome et al., 1993) or Q-plate (Helenes, 1986), or it was interpreted as part of the apical plate complex (Kim et al., 2005; Sarjeant, 1982). Just as its opposite apical plate 2′, this small plate forms the raised rim around the pore plate, and this plate is therefore regarded here as an integral part of the apical plate series and labelled accordingly to the Kofoidean system (Table 3).

In the hypotheca, different labels result from divergent interpretations of the two plates on the left side of the sulcal groove. The more posteriorly located, elongate plate is either considered the first antapical plate 1′′′′ (Kofoidean system) or the posterior intercalary plate 1p (in Taylor-Evitt notation). Subsequently, the small plate located more anteriorly is regarded as the first postcingular plate 1′′′ (Table 3) or plate Iu (in Taylor-Evitt notation). Rarely, it has been considered a sulcal plate (Kim et al., 2005). In Gonyaulacales, this plate is usually small, may not contact the cingulum (as it is the case in *L. polyedra*: Figs 5I, 6D) and may be located in the sulcus. However, the plate is generally referred to as the first postcingular plate regardless of its position (Fensome et al., 1993).

The overlap of specific plates is considered an important criterion to assess homologies between plates in different dinophytes. The first postcingular plate is, for example, recognised because it is overlapped by plate 1′′′′, and the latter is overlapped by plate 2′′′ (Figs 6B, D, S3). The third intercalary plate 3a overlaps the terminal precingular plate 6′′ in *L. polyedra*, just as plate 2a does in several species of *Gonyaulax* (Dodge, 1988). For *Gonyaulax elongata* (P.C.Reid) Ellegaard, Daugbjerg, Rochon, Jane Lewis & I.Harding, however, overlap in this area is inverted (Ellegaard et al., 2003).

The plate overlap pattern is rarely studied, but the present data are in large agreement with Dürr and Netzel (1974), variously reproduced as representative for Gonyaulacales in dinophyte text books such as Taylor (1987) and Fensome et al. (1993). However, it is important to note two deviating findings as worked out in the present study: a) Plate 1′′′′ overlaps plate 1′′′ (Fig. S3) and not in the reciprocal way (Dürr and Netzel, 1974), but this area of the cell wall is difficult to observe; b) plate 3a (plate 2a in Dürr and Netzel, 1974) overlaps plate 3′ (plate 4′ in Dürr and Netzel, 1974; Fig. S3), if overlap is discernible at all. Moreover, plates 1′′′′ and 2′′′′ are part of the postero-dextral daughter cell during cell division (Fig. S4), and Plate 1′′′′ is not of the antero-sinistral half as reported in Dürr and Netzel (1974). The distribution of plates along the fission line as described here for *L. polyedra* is also observed for species of *Gonyaulax* (Dodge, 1988).

4.3. Toxins

Toxin production of *L. polyedra* has been discussed controversially in the past. Dense blooms of *L. polyedra* have been linked to fish and/or benthic fauna kills (Torrey, 1902; Kofoid, 1911; Ballantine and Abbott, 1957; Reish, 1963; Marasović and Vukadin, 1982), but high cell densities during such blooms (e.g., 1.6×10^7 cells L^{-1}: Marasović and Vukadin, 1982) and low levels of oxygen make it likely that oxygen depletion was at least partly involved. Direct toxic effects of *L. polyedra* on mice was firstly reported by Schradie and Bliss (1962), who claimed the species to produce saxitoxin. However, this conclusion was doubted (Patton et al., 1967), and no saxitoxins were detected in subsequent studies (Bates et al., 1978). Based on the analysis of an extract obtained from a natural bloom sample dominated by *L. polyedra* Bruno et al. (1990) again claimed the dinophyte to produce PSP-like neurotoxic compounds. The limit of such studies is that toxin production of accompanying species cannot be excluded and at that time, chemical toxin analyses were not very reliable.

The present analysis of three clonal strains support the finding of Bates et al. (1978) that *L. polyedra* is not a producer of PSP toxins. Nevertheless, the species is known as a producer of YTXs, which are marine polyether toxins with low oral but high intraperitoneal toxicity when applied to mice (Paz et al., 2008). Additionally to *Protoceratium reticulatum* (Clap. & J.Lachm.) Buetschli and a few species of *Gonyaulax, L. polyedra* is a primary source organism for these toxins (Paz et al., 2004). However, strains with or without detectable YTXs are reported in the literature (Stobo et al., 2003; Howard et al., 2008). Our results confirm production of YTXs for *L. polyedra* strains from the type locality. All three strains lack yessotoxin (YTX, *m/z* 1141) and predominantly produce homo-YTX, as it is also reported for a few strains of *P. reticulatum* (Paz et al., 2007; Suzuki et al., 2007). A lack of YTX, and a high intraspecific variability in YTX profiles, have also been reported from *L. polyedra* strains from a Swedish Fjord (Peter et al., 2018). The relatively low cell quota obtained here and for further strains of *L. polyedra* (Paz et al., 2004; Howard et al., 2008; Peter et al., 2018) indicate a generally low toxin production potential compared to other species producing YTX. Cell quota of total YTXs up to 200 pg $cell^{-1}$ for *Gonyaulax spinifera* (Clap. & J.Lachm.) Diesing (Rhodes et al., 2006) or up to 70 pg $cell^{-1}$ for *P. reticulatum* (Paz et al., 2008) have been reported.

4.4. Molecular phylogenetics of Gonyaulacales

Various phylogenetic studies using DNA sequence data already have considered a reasonably representative set of Gonyaulacales for evolutionary inference (Kuno et al., 2010; Orr et al., 2012; Gu et al., 2013; Smith et al., 2017; Escalera et al., 2018; Mordret et al., 2018; Stephens et al., 2018; Gómez and Artigas, 2019; Li et al., 2019). However, a phylogenetic analysis is presented here based on a taxon sample representing the entire molecular diversity of Gonyaulacales as it is known today. The curated voucher list (Tab. S1) includes information about type material and geographic origin and may proof helpful as taxonomic backbone for the sample of future phylogenetic analyses.

Pyrocystales (Haeckel, 1894: 109) is the older name for the taxon under study here, in favour of Gonyaulacales (Taylor, 1980: [65,] 102–103). However, ICN Rec. 16A.1 indicates that the principle of priority does not apply obligatorily to names at ranks above the family and here, the broadly accepted taxon name provided by F.J.R. Taylor is used. Regarding the subdivision of Gonyaulacales, the present results confirm previous concepts and render them more precisely. Gómez (2012a), for example, recognised six taxa at family rank that are largely congruent to the present DNA tree (though adding then unrecognised †*Dapsilidinium*+*Grammatodininium*). As only significant difference, the molecular trees indicate a rather distinct phylogenetic status of Pyrodinioideae, whose members are still included in the equivalent of Ostreopsidoideae, stat. nov., by Gómez (2012a). The systematic placement of Thecadiniaceae has been uncertain for a long period of time (Fensome et al., 1993; Williams et al., 2017), and Moestrup and Calado (2018) placed the group even under Peridiniales not Gonyaulacales. Molecular trees like also the present one unequivocally show that Thecadiniaceae are an integral part of Gonyaulacales (Bolch and Campbell, 2004; Orr et al., 2012; Gottschling et al., 2020).

Molecular phylogenetics help to identify character polarity in gonyaulacalean dinophytes. Quinqueform and sexiform dinophytes (Fig. 2) do not constitute sister groups, as it is suggested by the dichotomous subdivision of Gonyaulacales into two taxa at equal rank (Fensome et al., 1993; Williams et al., 2017). In fact, the lineage with the quinqueform configuration (i.e., Pyrocystaceae) is supported as monophyletic by both Bayesian and ML approaches (deep blue clade in the Graphical Abstract), but the group exhibiting the sexiform configuration (i.e., the other gonyaulacalean dinophytes) is a paraphyletic grade rather than a clade (pale blue lineages in the Graphical Abstract). Thus,

Table 3
Selected compilation of plate formulas assigned to *L. polyedra*.

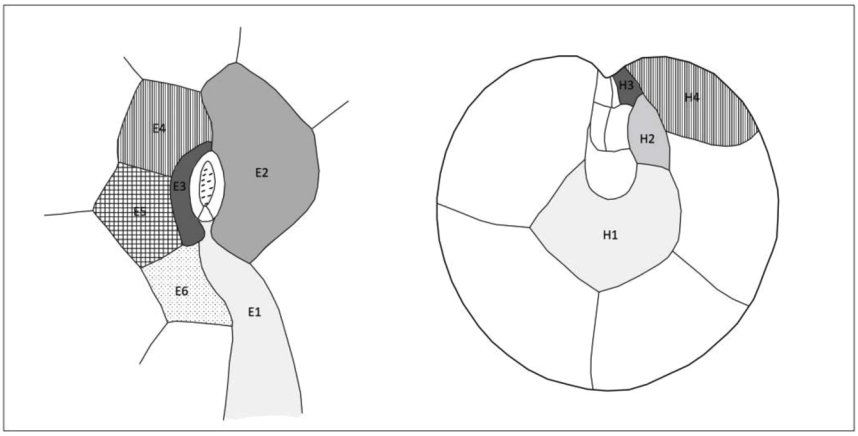

	E1	E2	E3	E4	E5	E6	H1	H2	H3	H4
Present	1'	2'	3'	1a	2a	3a	2""	1""	1"'	2"'
Kofoid 1911	1'	2'	4'	3'	1a	2a	1""	1p	1"'	2"'
Schiller 1933	1'	2'	4'	3'	1a	2a	1""	1p	1"'	2"'
Dürr & Netzel 1974	1'	2'	4'	3'	1a	2a	1""	1p	1"'	2"'
Kobayashi et al. 1981	1'	2'	4'	3'	1a	2a	1""	1p	1"'	2"'
Dodge 1982	1'	2'	4'	3'	1a	2a	1""	1p	1"'	2"'
Balech 1988	1'	2'	3'	1a	2a	3a	2""	1""	1"'	2"'
Dodge 1989	1'	2'	3'	1a	2a	3a	1""	1p	1"'	2"'
Steidinger & Tangen 1996	1'	2'	3'	1a	2a	3a	2""	1""	1"'	2"'
Kim et al. 2005	1'	2'	Q	3'	4'	5'	2""	1""	Ssa	1"'

two evolutionary steps can be inferred from the DNA trees (summarised in the Graphical Abstract): 1) Plates sp and 1‴ have been separated from each other in the last common ancestor of Gonyaulacales, and this apomorphy correspond to their monophyly in the molecular trees (the character stage is retained in a paraphyletic group); 2) during further evolution, plates 6‴ and 2⁗ have been separated as well (because of the contact between plates sp and 5‴; Fig. 2B), and this apomorphy of gonyaulacalean dinophytes with a quinqueform hypotheca supports the monophyly of Pyrocystaceae as demonstrated in the molecular trees.

With nesting *Centrodinium*, the monophyly of *Alexandrium* has recently been challenged (Gómez and Artigas, 2019; Li et al., 2019), and the best strategies to overcome the taxonomic confusion are currently discussed (Mertens et al., 2020). However, the phylogenetic status of *Alexandrium* has been rarely studied based on a representative taxon sample of the Gonyaulacales and particularly including the putative relatives, *Coolia* and *Ostreopsis*. The situation is anything but finally resolved, though our results agree with, for example, Orr et al. (2012) and Smith et al. (2017) indicating the possible paraphyly of *Alexandrium*. More research, preferably applying the battery of next generation sequencing tools available today, is necessary to entangle the difficult branch of Ostreopsidoideae, stat. nov., in the dinophyte tree of life.

The nomenclatural inconsistencies within Gonyaulacales (i.e., different names for the same species) may also refer to the problem that alternative taxonomic concepts exist for non-fossils and fossils and that different names are used in parallel also at the generic rank. Dual nomenclature may have been justified historically (Keupp, 1981; Head, 1996; Streng et al., 2002; Elbrächter et al., 2008; Ellegaard et al., 2018), as it originated at a time when the links between different developmental stages of life-history were not always clear in dinophytes. However, many such relationships have been uncovered in the past decades (Montresor et al., 1997; Gu et al., 2013), also in gonyaulacoid dinophytes (Ellegaard et al., 2002; Mertens et al., 2017; Li and Shin, 2019). Principle IV of the ICN (Turland et al., 2018) states that 'each taxonomic group … can bear only one correct name'. It is not only possible, but desirable and primarily the matter of taxonomic diligence, to overcome in future the Babylonian confusion regarding scientific names also for gonyaulacoid dinophytes, and particularly for the *Gonyaulax-*/†*Spiniferites*-schism as seen in the DNA tree.

5. Taxonomic activity

Biodiversity assessment in the microbial world and naming of species started in the late 18th and early 19th century, using light microscopy. Type material of these names consists either of illustrations or of specimens permanently mounted on glass slides. Many cannot be unambiguously determined, and DNA cannot be isolated from this material. To unambiguously resolve these names, the most powerful tool is epitypification. This consists in collecting new material as closely as possible to the type locality. The goal is to capture the original author's intent as inferred from the protologue, specimens and original illustrations. Clarifying the names is the basis for understanding dinophyte sexual reproduction, physiology, ecology, toxicology and the indicator potential of past temperature and water chemistry, last not least of harmful algae such as *L. polyedra*. However, there is already a number of examples with rather problematic epitype choices, not only amongst angiosperms (Mosyakin and McNeill, 2018) but also in the microbial world (Rindi et al., 2017; Žerdoner Čalasan et al., 2020) that the acceptance of the tool is challenged occasionally.

There is an ongoing debate into whether microbes are all cosmopolitan, and lack distinct distributions, or rather show various degrees of endemism (Žerdoner Čalasan et al., 2019; Gottschling et al., 2020, and cited references therein). The study of dinophyte taxa at their type

locality is considered key in order to resolve their taxonomic identity. However, not all authors seem to agree that distribution matters, and epitypes have been chosen from localities far distant from the original sites (e.g., material from Belize epitypifying original material from Kazakhstan: Faust and Steidinger, 1998; material from Kuwait epitypifying original material from California: Saburova et al., 2012; material from Tahiti epitypifying original material from Australia: Litaker et al., 2009). The possible disrupting potential and negative consequence for a stable taxonomy and nomenclature cannot yet be fully predicted, but caution when choosing an epitype is strongly advocated. This refers also to the fact that unfortunate choices cannot be unmade (ICN Art. 9.20) except through the elaborate process of taxonomic conservation (McNeill et al., 2015).

Most epitype material of dinophytes has been prepared from living material and if such strains are available in public strain collections, then they are available for further research. Therefore, some periodicals such as 'Protist' require deposition of strains, which is highly recommended if new taxa are described or their taxonomy is clarified. However, strains in cultivation may easily get lost due to technical problems, to rather complex growth requirements or potentially also due to programmed cell death. There is also ample evidence that many factors and processes over time alter various properties of microalgae that are maintained in laboratory strains (Lakeman et al., 2009, and references therein).

There is confidence that *L. polyedra* was recollected at the type locality in the Baltic Sea off Kiel more than 130 years after the description. Strain K3-G8, from which the epitype of *L. polyedra* was prepared, has been deposited at the Central Collection of Algal Cultures (CCAC 9295 B). The opportunity is taken and the name is epitypified with contemporary material (the SEM stub being the epitype is shown in the Graphical Abstract), realising what is here proposed to be the best practice approach:

> ***Lingulodinium polyedra* (F.Stein) J.D.Dodge**, Botanica Marina 32: [277,]291, Figs 1H–I, 34–38. 1989. *Gonyaulax polyedra* F.Stein, Der Organismus der Flagellaten nach eigenen Forschungen in systematischer Reihenfolge bearbeitet 3.2: 13, pl. IV 7–9. 1883.–Type [non-fossil]: Baltic Sea, off Germany. Schleswig-Holstein, Kiel Fjord, probably late summer 1879 (Wentzel, 1885): F. von Stein s.n.; **lectotype, designated here**: [illustration] pl. IV 8! in Stein (1883); **epitype, designated here**: Baltic Sea, off Germany. Schleswig-Holstein, Kiel Fjord, 9th September 2019: [SEM stub] U. Tillmann, M. Gottschling & H. Gu [U. Tillmann K3-G8] s.n. (CEDiT2020**E**108!). Formol-fixed material is also available (CEDit2020**RM**109). [http://phycobank.org/102192].

Three names as used in the present study were not available at the rank of a subfamily so far, and the necessary new taxonomic states are here provided:

> **Ostreopsidoideae Gottschling, Tillmann & Elbr., stat. nov.** Basionym: Ostreopsidaceae Er.Lindem., nom. corr. (ICN Art. 18.4), in Engl. & Prantl, Die natürlichen Pflanzenfamilien ed. 2 2: [35], 96. 1928. [http://phycobank.org/102193].
>
> **Pyrocystoideae Gottschling, Tillmann & Elbr., stat. nov.** Basionym: Pyrocysteae F.Schütt in Engl. & Prantl, Die natürlichen Pflanzenfamilien 1 (1b): 3. 1896. [http://phycobank.org/102194].
>
> **Pyrophacoideae Gottschling, Tillmann & Elbr., stat. nov.** Basionym: Pyrophacaceae Er.Lindem. in Engl. & Prantl, Die natürlichen Pflanzenfamilien ed. 2 2: [34], 96. 1928. [http://phycobank.org/102195].

Declaration of Competing Interest

The authors declare that they have no known competing financial interests or personal relationships that could have appeared to influence the work reported in this paper.

Acknowledgements

We thank Hans-Joachim Esser (Munich) and Wolf-Henning Kusber (Berlin) for the discussion of dinophyte nomenclature and taxonomy. Annegret Müller and Thomas Max (AWI) are thanked for technical support. This work was supported by the PACES research program of the Alfred Wegener Institute as part of the Helmholtz Foundation initiative in Earth and Environment. ME gratefully acknowledges the ongoing support of the Alfred-Wegener-Institut, Wattenmeerstation Sylt.

Supplementary materials

Supplementary material associated with this article can be found, in the online version, at doi:10.1016/j.hal.2020.101956.

References

Álvarez, G., Uribe, E., Regueiro, J., Blanco, J., Fraga, S., 2016. *Gonyaulax taylorii*, a new yessotoxins-producer dinoflagellate species from Chilean waters. Harmful Algae 58, 8–15.
Anderson, D.M., Alpermann, T.J., Cembella, A.D., Collos, Y., Masseret, E., Montresor, M., 2012. The globally distributed genus *Alexandrium*: multifaceted roles in marine ecosystems and impacts on human health. Harmful Algae 14, 10–35.
Balech, E., 1988. Los Dinoflagelados Del Atlantico Sudoccidental. Ministerio de Agricultura, Pesca y Alimentación, Madrid.
Balech, E., 1995. The Genus *Alexandrium* Halim (Dinoflagellata). Sherkin Island Marine Station, Sherkin Island.
Ballantine, D., Abbott, B.C., 1957. Toxic marine flagellates: their occurrence and physiological effects on animals. J. Gen. Microbiol. 16, 274–281.
Bates, H.A., Kostriken, R., Rapoport, H., 1978. The occurrence of saxitoxin and other toxins in various dinoflagellates. Toxicon 16, 595–601.
Bergsten, J., 2005. A review of long-branch attraction. Cladistics 21, 163–193.
Bolch, C.J.S., Campbell, C.N., 2004. Morphology and phylogenetic affinities of *Thecadinium foveolatum* sp. nov. (Dinophyceae: Thecadiniaceae), a new marine benthic dinoflagellate from the West of Scotland. Eur. J. Phycol. 39, 351–360.
Bruno, M., Gucci, P.M.B., Pierdominici, E., Ioppolo, A., Volterra, L., 1990. Presence of saxitoxin in toxic extracts from *Gonyaulax polyedra*. Toxicon 28, 1113–1116.
Carbonell-Moore, M.C., 1996. On *Spiraulax jolliffei* (Murray et Whitting) Kofoid and *Gonyaulax fusiformis* Graham (Dinophyceae). Botanica Marina 39, 347–370.
Carbonell-Moore, C., Mertens, K.N., 2020. On *Acanthogonyaulax spinifera* (Dinophyceae). Phycologia 59, 456–459.
Chomérat, N., Gatti, C.M.I., Nézan, E., Chinain, M., 2017. Studies on the benthic genus *Sinophysis* (Dinophysales, Dinophyceae) II. *S. canaliculata* from Rapa Island (French Polynesia). Phycologia 56, 193–203.
Craveiro, S.C., Daugbjerg, N., Moestrup, Ø., Calado, A.J., 2017. Studies on *Peridinium aciculiferum* and *Peridinium malmogiense* (=*Scrippsiella hangoei*): comparison with *Chimonodinium lomnickii* and description of *Apocalathium gen. nov.* (Dinophyceae). Phycologia 56, 21–35.
Daugbjerg, N., Hansen, G., Larsen, J., Moestrup, Ø, 2000. Phylogeny of some of the major genera of dinoflagellates based on ultrastructure and partial LSU rDNA sequence data, including the erection of three new genera of unarmoured dinoflagellates. Phycologia 39, 302–317.
Dodge, J.D., 1988. An SEM study of thecal division in *Gonyaulax* (Dinophyceae). Phycologia 27, 241–247.
Dodge, J.D., 1989. Some revisions of the family Gonyaulacaceae (Dinophyceae) based on a scanning electron microscope study. Botanica Marina 32, 275–298.
Dodge, J.D., Hermes, H.B., 1981. A scanning electron microscopical study of the apical pores of marine dinoflagellates (Dinophyceae). Phycologia 20, 424–430.
Dürr, G., Netzel, H., 1974. The fine-structure of cell surface in *Gonyaulax polyedra* (Dinoflagellata). Cell Tissue Res. 150, 21–41.
Elbrächter, M., Gottschling, M., 2015. (2383) Proposal to reject the name Goniodomataceae (Dinophyceae). Taxon 64, 1052–1053.
Elbrächter, M., Gottschling, M., Hildebrand-Habel, T., Keupp, H., Kohring, R., Lewis, J., Meier, K.J.S., Montresor, M., Streng, M., Versteegh, G.J.M., Willems, H., Zonneveld, K.A.F., 2008. Establishing an Agenda for Calcareous Dinoflagellate Research (Thoracosphaeraceae, Dinophyceae) including a nomenclatural synopsis of generic names. Taxon 57, 1289–1303.
Ellegaard, M., Daugbjerg, N., Rochon, A., Lewis, J., Harding, I., 2003. Morphological and LSU rDNA sequence variation within the *Gonyaulax spinifera–Spiniferites* group (Dinophyceae) and proposal of *G. elongata* comb. nov. and *G. membranacea* comb. nov. Phycologia 42, 151–164.
Ellegaard, M., Head, M.J., Versteegh, G.J.M., 2018. Linking biological and geological data on dinoflagellates using the genus *Spiniferites* as an example: the implications of species concepts, taxonomy and dual nomenclature. Palynology 42, 221–230.
Ellegaard, M., Lewis, J., Harding, I., 2002. Cyst-theca relationship, life cycle, and effects of temperature and salinity on the cast morphology of *Gonyaulax baltica* sp. nov. (Dinophyceae) from the Baltic Sea area. J. Phycol. 38, 775–789.

Escalera, L., Italiano, A., Pistocchi, R., Montresor, M., Zingone, A., 2018. *Gonyaulax hyalina* and *Gonyaulax fragilis* (Dinoflagellata), two names associated with 'mare sporco', indicate the same species. Phycologia 57, 453–464.
Evitt, W.R., 1985. Sporopollenin dinoflagellate cysts. Their Morphology and Interpretation. Hart Graphics, Austin, pp. vii–xiii, 84–90, 284–285, 299–301.
Faust, M.A., Litaker, R.W., Vandersea, M.W., Kibler, S.R., Tester, P.A., 2005. Dinoflagellate diversity and abundance in two Belizean coral-reef mangrove lagoons: a test of Margalef's Mandala. Atoll Res. Bull. 534, 103–131.
Faust, M.A., Steidinger, K.A., 1998. *Bysmastrum* gen. nov. (Dinophyceae) and three new combinations for benthic scrippsielloid species. Phycologia 37, 47–52.
Fensome, R.A., Taylor, F.J.R., Norris, G., Sarjeant, W.A.S., Wharton, D.I., Williams, G.L., 1993. A classification of living and fossil dinoflagellates. Micropaleontology Special Publication Number 7, 1–245.
Gómez, F., 2012a. A checklist and classification of living dinoflagellates (Dinoflagellata, Alveolata). CICIMAR Oceánides 27, 65–140.
Gómez, F., 2012b. A quantitative review of the lifestyle, habitat and trophic diversity of dinoflagellates (Dinoflagellata, Alveolata). System. Biodivers. 10, 267–275.
Gómez, F., Artigas, L.F., 2019. Redefinition of the dinoflagellate genus *Alexandrium* based on *Centrodinium*: reinstatement of *Gessnerium* and *Protogonyaulax*, and *Episemicolon* gen. nov. (Gonyaulacales, Dinophyceae). Hindawi J. Mar. Biol. 2019, 1284104.
Gottschling, M., Chacón, J., Žerdoner Čalasan, A., Neuhaus, St, Kretschmann, J., Stibor, H., John, U., 2020. Phylogenetic placement of environmental sequences using taxonomically reliable databases helps to rigorously assess dinophyte biodiversity in Bavarian lakes (Germany). Freshw. Biol. 65, 193–208.
Gottschling, M., Elbrächter, M., 2015. (2382) Proposal to conserve the name *Scrippsiella* against *Heteraulacus* and *Goniodoma* (Thoracosphaeraceae, Dinophyceae). Taxon 64, 1051–1052.
Gottschling, M., Keupp, H., Plötner, J., Knop, R., Willems, H., Kirsch, M., 2005. Phylogeny of calcareous dinoflagellates as inferred from ITS and ribosomal sequence data. Mol. Phylogenet. Evol. 36, 444–455.
Gottschling, M., Söhner, S., Zinßmeister, C., John, U., Plötner, J., Schweikert, M., Aligizaki, K., Elbrächter, M., 2012. Delimitation of the Thoracosphaeraceae (Dinophyceae), including the calcareous dinoflagellates, based on large amounts of ribosomal RNA sequence data. Protist 163, 15–24.
Gottschling, M., Tillmann, U., Kusber, W.-.H., Hoppenrath, M., Elbrächter, M., 2018. A Gordian knot: nomenclature and taxonomy of *Heterocapsa triquetra* (Peridiniales: Heterocapsaceae). Taxon 67, 179–185.
Gu, H., Kirsch, M., Zinßmeister, C., Söhner, S., Meier, K.J.S., Liu, T., Gottschling, M., 2013. Waking the dead: morphological and molecular characterization of extant †*Posoniella tricarinelloides* (Thoracosphaeraceae, Dinophyceae). Protist 164, 583–597.
Haeckel, E.H.P.A., 1894. Systematische Phylogenie der Protisten und Pflanzen. Reimer, Berlin.
Hällfors, G., 2004. Checklist of Baltic Sea phytoplankton species (including some heterotrophic protistan groups). Balt. Sea Environ. Proc. 95, 1–208.
Haxo, F.T., Sweeney, B.M., 1955. Bioluminiszenz in *Gonyaulax polyedra*. In: Johnson, F. H. (Ed.), The Luminiscence of Biological Systems. American Association for Advancement of Science, Washington D.C, pp. 415–420.
Head, M.J., 1996. Chapter 30. Modern dinoflagellate cysts and their biological affinities. In: Jansonius, J., McGregor, D.C. (Eds.), Palynology: Principles and Applications. Publishers Press, Salt Lake City, pp. 1197–1248.
Head, M.J., Edwards, L.E., Garrett, J.K., Lentin, J.K., Marret, F., Matsuoka, K., Matthiessen, J., O'Mahony, J., Sun, X., Verteuil, L.d., Zevenboom, D, 1994. A forum on Neogene and Quaternary dinoflagellate cysts. The edited transcript of a round table discussion held at the Third Workshop on Neogene and Quaternary dinoflagellates; with taxonomic appendix. Palynology 17, 201–239.
Helenes, J., 1986. Some variation in the paratabulation of gonyaulacoid dinoflagellates. Palynology 10, 73–110.
Holmes, M.J., Brust, A., Lewis, R.J., 2014. Dinoflagellate toxins: an overview. In: Botana, L.M. (Ed.), Seafood and Freshwater Toxins. Pharmacology, Phsiology, and Detection. CRC Press, Boca Raton, pp. 3–38.
Howard, M.D.A., Silver, M., Kudela, R.M., 2008. Yessotoxin detected in mussel (*Mytilus californicus*) and phytoplankton samples from the US west coast. Harmful Algae 7, 646–652.
Katoh, K., Standley, D.M., 2013. MAFFT multiple sequence alignment software version 7: improvements in performance and usability. Mol. Biol. Evol. 30, 772–780.
Keller, M.D., Selvin, R.C., Claus, W., Guillard, R.R.L., 1987. Media for the culture of oceanic ultraphytoplankton. J. Phycol. 23, 633–638.
Keupp, H., 1981. Die kalkigen Dinoflagellaten-Zysten der borealen Unter-Kreide (Unter-Hauterivium bis Unter-Albium). Facies 5, 1–190.
Kim, K.-.Y., Yoshida, M., Kim, C.-.H., 2005. Morphological variation of *Lingulodinium polyedrum* (Dinophyceae) in culture specimens and reinterpretation of the thecal formula. Algae 20, 299–304.
Kobayashi, S., Matsuoka, K., Iizuka, S., 1981. 大村湾底泥中からの *Gonyaulax polyedra* STEIN シストの発見. Bulletin of the Plankton Society of Japan 28, 53–57.
Kofoid, C.A., 1909. On *Peridinium steinii* Jörgensen, with a note on the nomenclature of the skeleton of the Peridinidae. Archiv für Protistenkunde 16, 25–47.
Kofoid, C.A., 1911. Dinoflagellata of the San Diego region, IV: the genus *Gonyaulax*, with notes on its skeletal morphology, and a discussion of its generic and specific characters. Univ. Calif. Publ. Zool. 8, 187–286.
Kremp, A., Tahvanainen, P., Litaker, W., Krock, B., Suikkanen, S., Leaw, C.P., Tomas, C., 2014. Phylogenetic relationships, morphological variation, and toxin patterns in the *Alexandrium ostenfeldii* (Dinophyceae) complex: implications for species boundaries and identities. J. Phycol. 50, 81–100.
Kretschmann, J., Elbrächter, M., Zinßmeister, C., Söhner, S., Kirsch, M., Kusber, W.-.H., Gottschling, M., 2015. Taxonomic clarification of the dinophyte *Peridinium acuminatum* Ehrenb.,≡*Scrippsiella acuminata*, comb. nov. (Thoracosphaeraceae, Peridiniales). Phytotaxa 220, 239–256.
Kretschmann, J., Žerdoner Čalasan, A, Kusber, W.-.H., Gottschling, M., 2018. Still curling after all these years: *Glenodinium apiculatum* Ehrenb. (Peridiniales, Dinophyceae) repeatedly found at its type locality in Berlin (Germany). System. Biodivers. 16, 200–209.
Kuno, S., Kamikawa, R., Yoshimatsu, S., Sagara, T., Nishio, S., Sako, Y., 2010. Genetic diversity of *Gambierdiscus* spp. (Gonyaulacales, Dinophyceae) in Japanese coastal areas. Phycological Res. 58, 44–52.
Lakeman, M.B., von Dassow, P., Cattolico, R.A., 2009. The strain concept in phytoplankton ecology. Harmful Algae 8, 746–758.
Lewis, J., Burton, P., 1988. A study of newly excysted cells of *Gonyaulax polyedra* (Dinophyceae) by electron microscopy. British Phy. J. 23, 49–60.
Lewis, J., Hallett, R., 1997. *Lingulodinium polyedrum* (*Gonyaulax polyedra*) a blooming dinoflagellate. Oceanography and Marine Biology 35, 97–161.
Li, Z., Mertens, K.N., Nézan, E., Chomérat, N., Bilien, G., Iwataki, M., Shin, H.H., 2019. Discovery of a new clade nested within the genus *Alexandrium* (Dinophyceae): morpho-molecular characterization of *Centrodinium punctatum* (Cleve) FJR Taylor. Protist 170, 168–186.
Li, Z., Oh, S.J., Park, J.-.W., Lim, W.-.A., Shin, H.H., 2017. Cyst-motile stage relationship, morphology and phylogeny of a new chain-forming, marine dinoflagellate *Grammatodinium tongyeonginum* gen. & sp. nov. from Korea. Phycologia 56, 430–443.
Li, Z., Shin, H.H., 2019. Morphology, phylogeny and life cycle of *Fragilidium mexicanum* Balech (Gonyaulacales, Dinophyceae). Phycologia 58, 419–432.
Lim, A.S., Jeong, H.J., Kwon, J.E., Lee, S.Y., Kim, J.H., 2018. *Gonyaulax whaseongensis* sp. nov. (Gonyaulacales, Dinophyceae), a new phototrophic species from Korean coastal waters. J. Phycol. 54, 923–928.
Litaker, R.W., Vandersea, M.W., Faust, M.A., Kibler, S.R., Chinain, M., Holmes, M.J., Holland, W.C., Tester, P.A., 2009. Taxonomy of *Gambierdiscus* including four new species, *Gambierdiscus caribaeus, Gambierdiscus carolinianus, Gambierdiscus carpenteri* and *Gambierdiscus ruetzleri* (Gonyaulacales, Dinophyceae). Phycologia 48, 344–390.
Luo, Z., Lim, Z.F., Mertens, K.N., Krock, B., Teng, S.T., Tan, T.H., Leaw, C.P., Lim, P.T., Gu, H., 2019. Attributing *Ceratocorys, Pentaplacodinium* and *Protoceratium* to Protoceratiaceae (Dinophyceae), with descriptions of *Ceratocorys malayensis* sp. nov. and *Pentaplacodinium usupianum* sp. nov. Phycologia 59, 6–23.
Marasović, I., Vukadin, I., 1982. "Red tide" in the Vranjic basin (Kaštela Bay). Bilješke - Notes. Institut za Oceanografiju i Ribarstvo — Split 1–7.
McNeill, J., Redhead, S.A., Wiersema, J.H., 2015. Guidelines for proposals to conserve or reject names. Taxon 64, 163–166, 845.
Mertens, K.N., Adachi, M., Anderson, D.M., Band-Schmidt, C.J., Bravo, I., Brosnahan, M. L., Bolch, C.J.S., Calado, A.J., Carbonell-Moore, M.C., Chomérat, N., Elbrächter, M., Figueroa, R.I., Fraga, S., Gárate-Lizárraga, I., Garcés, E., Gu, H., Hallegraeff, G., Hess, Ph., Hoppenrath, M., Horiguchi, T., Iwataki, M., John, U., Kremp, A., Larsen, J., Leaw, C.P., Li, Z., Lim, P.T., Litaker, W., MacKenzie, L., Masseret, E., Matsuoka, K., Moestrup, Ø., Montresor, M., Nagai, S., Nézan, E., Nishimura, T., Okolodkov, Y.B., Orlova, T.Yu., Reñé, A, Sampedro, N, Satta, C.T., Shin, H.H., Siano, R., Smith, K.F., Steidinger, K., Takanoa, Y., Tillmann, U., Wolny, J., Yamaguchi, A., Murray, Sh, 2020. Morphological and phylogenetic data do not support the split of *Alexandrium* into four genera. Harmful Algae 98.
Mertens, K.N., Carbonell-Moore, M.C., Pospelova, V., Head, M.J., Highfield, A., Schroeder, D., Gu, H., Andree, K.B., Fernandez, M., Yamaguchi, A., Takano, Y., Matsuoka, K., Nézan, E., Bilien, G., Okolodkov, Y., Koike, K., Hoppenrath, M., Pfaff, M., Pitcher, G., Al-Muftah, A., Rochon, A., Lim, P.T., Leaw, C.P., Lim, Z.F., Ellegaard, M., 2018. *Pentaplacodinium saltonense* gen. et sp. nov. (Dinophyceae) and its relationship to the cyst-defined genus *Operculodinium* and yessotoxin-producing *Protoceratium reticulatum*. Harmful Algae 71, 57–77.
Mertens, K.N., Takano, Y., Gu, H., Bagheri, S., Pospelova, V., Pienkowski, A.J., Leroy, S. A.G., Matsuoka, K., 2017. Cyst-theca relationship and phylogenetic position of *Impagidinium caspienense* incubated from Caspian Sea surface sediments: relation to *Gonyaulax baltica* and evidence for heterospory within gonyaulacoid dinoflagellates. J. Eukaryot. Microbiol. 64, 829–842.
Miller, M.A., Pfeiffer, W., Schwartz, T., 2010. Creating the CIPRES Science Gateway for inference of large phylogenetic trees. Proceedings of the Gateway Computing Environments Workshop (GCE) 1–8.
Moestrup, Ø., Calado, A.J., 2018. Dinophyceae. Springer, Berlin.
Montresor, M., Janofske, D., Willems, H., 1997. The cyst-theca relationship in *Calciodinellum operosum* emend. (Peridiniales, Dinophyceae) and a new approach for the study of calcareous cysts. J. Phycol. 33, 122–131.
Mordret, S., Piredda, R., Vaulot, D., Montresor, M., Kooistra, W.H.C.F., Sarno, D., 2018. DINOREF: a curated dinoflagellate (Dinophyceae) reference database for the 18S rRNA gene. Mol. Ecol. Resour. 18, 974–987.
Mosyakin, S.L., McNeill, J., 2018. On the nomenclature of *Chenopodium pallidum* and *Atriplex schugnanica* (Chenopodiaceae / Amaranthaceae sensu APG) and the perils of epitypification. Phytotaxa 376, 133–137.
Nehring, S., 1994. Spatial distribution of dinoflagellate resting cysts in recent sediments of Kiel Bight, Germany (Baltic Sea). Ophelia 39, 137–158.
Nehring, S., 1997. Dinoflagellate resting cysts from recent German coastal sediments. Botanica Marina 40, 307–324.
Nordli, E., 1951. Resting spores in *Gonyaulax polyedra* Stein. Nytt Magasin for Naturvitenskapene 88, 207–212.
Orr, R.J.S., Murray, S.A., Stüken, A., Rhodes, L., Jakobsen, K.S., 2012. When naked became armored: an eight-gene phylogeny reveals monophyletic origin of theca in dinoflagellates. PLoS ONE 7, e50004.

Parsons, M.L., Aligizaki, K., Bottein, M.Y.D., Fraga, S., Morton, S.L., Penna, A., Rhodes, L., 2012. *Gambierdiscus* and *Ostreopsis*: reassessment of the state of knowledge of their taxonomy, geography, ecophysiology, and toxicology. Harmful Algae 14, 107–129.
Patton, S., Chandler, P.T., Kalan, E.B., Loeblich III, A.R., Fuller, G., Benson, A.A., 1967. Food value of red tide (*Gonyaulax polyedra*). Science 158, 789–790.
Paz, B., Daranas, A.H., Norte, M., Riobó, P., Franco, J.M., Fernández, J.J., 2008. Yessotoxins, a group of marine polyether toxins: an overview. Mar. Drugs 6, 73–102.
Paz, B., Riobó, P., Fernández, A.L., Fraga, S., Franco, J.M., 2004. Production and release of yessotoxins by the dinoflagellates *Protoceratium reticulatum* and *Lingulodinium polyedrum* in culture. Toxicon 44, 251–258.
Paz, B., Riobó, P., Ramilo, I., Franco, J.M., 2007. Yessotoxins profile in strains of *Protoceratium reticulatum* from Spain and USA. Toxicon 50, 1–17.
Peter, C., Krock, B., Cembella, A., 2018. Effects of salinity variation on growth and yessotoxin composition in the marine dinoflagellate *Lingulodinium polyedra* from a Skagerrak fjord system (western Sweden). Harmful Algae 78, 9–17.
Prud'homme van Reine, W.F., 2017. Report of the Nomenclature Committee for Algae: 15. Taxon 66, 191–192.
Reish, D.J., 1963. Mass mortality of marine organisms attributed to the "red tide" in Southern California. Calif. Fish. Game 49, 265–270.
Rhodes, L., McNabb, P., de Salas, M., Briggs, L., Beuzenberg, V., Gladstone, M., 2006. Yessotoxin production by *Gonyaulax spinifera*. Harmful Algae 5, 148–155.
Rhodes, L., Wood, S., 2014. Micro-algal and cyanobacterial producers of biotoxins. In: Rossini, G.P (Ed.), Toxins and Biologically Active Compounds from Microalgae. CRC Press, Boca Raton, pp. 21–50.
Rindi, F., Ryšánek, D., Škaloud, P., 2017. Problems of epitypification in morphologically simple green microalgae: a case study of two widespread species of *Klebsormidium* (Klebsormidiophyceae, Streptophyta). Fottea 17, 78–88.
Ronquist, F., Teslenko, M., van der Mark, P., Ayres, D.L., Darling, A., Höhna, S., Larget, B., Liu, L., Suchard, M.A., Huelsenbeck, J.P., 2012. MrBayes 3.2: efficient Bayesian phylogenetic inference and model choice across a large model space. Syst. Biol. 61, 539–542.
Saburova, M., Chomérat, N., Hoppenrath, M., 2012. Morphology and SSU rDNA phylogeny of *Durinskia agilis* (Kofoid & Swezy) comb. nov. (Peridiniales, Dinophyceae), a thecate, marine, sand-dwelling dinoflagellate formerly classified within *Gymnodinium*. Phycologia 51, 287–302.
Sala-Pérez, M., Alpermann, T.J., Krock, B., Tillmann, U., 2016. Growth and bioactive secondary metabolites of arctic *Protoceratium reticulatum* (Dinophyceae). Harmful Algae 55, 85–96.
Saldarriaga, J.F., Taylor, F.J.R., Keeling, P.J., Cavalier-Smith, T., 2001. Dinoflagellate nuclear SSU rRNA phylogeny suggests multiple plastid losses and replacements. J. Mol. Evol. 53, 204–213.
Sarjeant, W.A.S., 1982. Dinoflagellate cyst terminology: a discussion and proposals. Can. J. Bot. 60, 922–945.
Schmitter, R.E., 1971. Fine structure of *Gonyaulax polyedra*, a bioluminescent marine dinoflagellate. J. Cell. Sci. 9, 147–173.
Schradie, J., Bliss, C.A., 1962. The cultivation and toxicity of *Gonyaulax polyedra*. Lloydia 25, 214–221.
Smith, K.F., Kohli, G.S., Murray, S.A., Rhodes, L.L., 2017. Assessment of the metabarcoding approach for community analysis of benthic-epiphytic dinoflagellates using mock communities. N. Z. J. Mar. Freshwater Res. 51, 555–576.
Soliño, L., Costa, P.R., 2018. Differential toxin profiles of ciguatoxins in marine organisms: chemistry, fate and global distribution. Toxicon 150, 124–143.
Stamatakis, A., 2014. RAxML version 8: a tool for phylogenetic analysis and post-analysis of large phylogenies. Bioinformatics 30, 1312–1313.
Steidinger, K.A., Tangen, K., 1996. 3. Dinoflagellates. In: Tomas, C.R. (Ed.), Identifying Marine Diatoms and Dinoflagellates. Academic Press, San Diego, pp. 387–583.
Stein, S.F.N.R.v., 1883. Der Organismus der Infusionsthiere nach eigenen Forschungen in systematischer Reihenfolge bearbeitet 3.2. Engelmann, Leipzig.
Stephens, T.G., Ragan, M.A., Bhattacharya, D., Chan, C.X., 2018. Core genes in diverse dinoflagellate lineages include a wealth of conserved dark genes with unknown functions. Sci. Rep. 8, 17175.
Stobo, L.A., Lewis, J., Quilliam, M.A., Hardstaff, W.R., Gallacher, S., Webster, L., Smith, E.A., McKenzie, M., 2003. Detection of yessotoxin in UK and Canadian isolates of phytoplankton and optimization and validation of LC-MS methods. In: Bates, S.S (Ed.), Detection of yessotoxin in UK and Canadian isolates of phytoplankton and optimization and validation of LC-MS methods. Proceedings of the Eighth Canadian workshop on harmful marine algae 8–14.
Streng, M., Hildebrand-Habel, T., Willems, H., 2002. Revision of the genera *Sphaerodinella* Keupp and Versteegh, 1989 and *Orthopithonella* Keupp in Keupp and Mutterlose, 1984 (Calciodinelloideae, calcareous dinoflagellate cysts). J. Paleontol. 76, 397–407.
Sunesen, I., Rodríguez, F., Tardivo Kubis, J.A., Aguiar Juárez, D., Risso, A., Lavigne, A.S., Wietkamp, St., Tillmann, U., Sar, E.A., 2020. Morphological and molecular characterization of *Heterocapsa claromecoensis* sp. nov. (Peridiniales, Dinophyceae) from Buenos Aires coastal waters (Argentina). Eur. J. Phycol. 55 (4), 490–506.
Suzuki, T., Horie, Y., Koike, K., Satake, M., Oshima, Y., Iwataki, M., Yoshimatsu, S., 2007. Yessotoxin analogues in several strains of *Protoceratium reticulatum* in Japan determined by liquid chromatography-hybrid triple quadrupole/linear ion trap mass spectrometry. J. Chromatogr. A. 1142, 172–177.
Taylor, F.J.R., 1980. On dinoflagellate evolution. Biosystems 13, 65–108.
Taylor, F.J.R., 1987. Dinoflagellate morphology. In: Taylor, F.J.R. (Ed.), The Biology of Dinoflagellates. Blackwell, Oxford, pp. 24–91.
Taylor, F.J.R., 1990. 24 Phylum Dinoflagellata. In: Margulis, L., Corliss, J.O., Melkonian, M., Chapman, D.J. (Eds.), Handbook of Protoctista. The Structure, Cultivation, Habitats and Life Histories of the Eukaryotic Microorganisms and Their Descendants Exclusive of animals, Plants and Fungi. A Guide to the Algae, Ciliates, Foraminifera, Sporozoa, Water Molds, Slime Molds and the Other Protoctists. Jones and Bartlett, Boston, pp. 419–437.
Tillmann, U., Elbrächter, M., Krock, B., John, U., Cembella, A., 2009. *Azadinium spinosum* gen. et sp. nov. (Dinophyceae) identified as a primary producer of azaspiracid toxins. Eur. J. Phycol. 44, 63–79.
Tillmann, U., Hoppenrath, M., Gottschling, M., 2019. Reliable determination of *Prorocentrum micans* Ehrenb (Prorocentrales, Dinophyceae) based on newly collected material from the type locality. Eur. J. Phy. 54, 417–431.
Tillmann, U., Hoppenrath, M., Gottschling, M., Kusber, W.-.H., Elbrächter, M., 2017. Plate pattern clarification of the marine dinophyte *Heterocapsa triquetra* sensu Stein (Dinophyceae) collected at the Kiel Fjord (Germany). J. Phycol. 53, 1305–1324.
Tillmann, U., Salas, R., Gottschling, M., Krock, B., O'Driscoll, D., Elbrächter, M., 2012. *Amphidoma languida* sp. nov. (Dinophyceae) reveals a close relationship between *Amphidoma* and *Azadinium*. Protist 163, 701–719.
Tillmann, U., Wietkamp, S., Krock, B., Tillmann, A., Voss, D., Gu, H., 2020. Amphidomataceae (Dinophyceae) in the western Greenland area, including description of *Azadinium perforatum* sp. nov. Phycologia 59, 63–88.
Torrey, H.B., 1902. An unusual occurrence of Dinoflagellata on the California coast. Am. Nat. 36, 187–192.
Tubaro, A., Dell'Ovo, V., Sosa, S., Florio, C., 2010. Yessotoxins: a toxicological overview. Toxicon 56, 163–172.
Turland, N.J., Wiersema, J.H., Barrie, F.R., Greuter, W., Hawksworth, D.L., Herendeen, P.S., Knapp, S., Kusber, W.-.H., Li, D.-.Z., Marhold, K., May, T.W., McNeill, J., Monro, A.M., Prado, J., Price, M.J., Smith, G.F., 2018. International Code of Nomenclature for algae, fungi, and plants (Shenzhen Code) adopted by the Nineteenth International Botanical Congress Shenzhen, China, July 2017. Koeltz, Glashütten.
Van de Waal, D.B., Tillmann, U., Martens, H., Krock, B., van Scheppingen, Y., John, U., 2015. Characterization of multiple isolates from an *Alexandrium ostenfeldii* bloom in The Netherlands. Harmful Algae 49, 94–104.
Wall, D., Dale, B., 1967. The resting cysts of modern marine dinoflagellates and their palaeontological significance. Rev. Palaeobot. Palynol. 2, 349–354.
Wall, D., Dale, B., Harada, K., 1973. Descriptions of new fossil dinoflagellates from the Late Quaternary of the Black Sea. Micropaleontology 19, 18–31.
Wentzel, J., 1885. Hofrath Friedrich Ritter von Stein. Lotos - Zeitschrift für Naturwissenschaften 34. XXIII–XXXII.
Wietkamp, S., Krock, B., Gu, H., Voss, D., Klemm, K., Tillmann, U., 2019. Occurrence and distribution of Amphidomataceae (Dinophyceae) in Danish coastal waters of the North Sea, the Limfjord and the Kattegat/Belt area. Harmful Algae 88, 101637.
Williams, G.L., Fensome, R.A., MacRae, R.A., 2017. The Lentin and Williams Index of fossil dinoflagellates. 2017 Edition.
Žerdoner Čalasan, A., Kretschmann, J., Filipowicz, N.H., Irimia, R.-.E., Kirsch, M., Gottschling, M., 2019. Towards global distribution maps of unicellular organisms such as calcareous dinophytes based on DNA sequence information. Marine Biodiversity 49, 749–758.
Žerdoner Čalasan, A., Kretschmann, J., Gottschling, M., 2020. Contemporary integrative taxonomy for sexually deprived protists: a case study of *Trachelomonas* (Euglenaceae) from western Ukraine. Taxon 69, 28–42.
Zhang, W., Li, Z., Mertens, K.N., Derrien, A., Pospelova, V., Carbonell-Moore, M.C., Bagheri, S., Matsuoka, K., Shin, H.H., Gu, H., 2020. Reclassification of *Gonyaulax verior* (Gonyaulacales, Dinophyceae) as *Sourniaea diacantha* gen. et comb. nov. Phycologia 59, 246–260.
Zinßmeister, C., Söhner, S., Facher, E., Kirsch, M., Meier, K.J.S., Gottschling, M., 2011. Catch me if you can: the taxonomic identity of *Scrippsiella trochoidea* (F.Stein) A.R. Loebl. (Thoracosphaeraceae, Dinophyceae). System. Biodivers. 9, 145–157.